Hardware Implementation of Filtering Based Sidelobe Suppression for Spectrally Agile Multicarrier based Cognitive Radio Systems

by

AMIT SAIL
B.E.(Electronics and Telecommunication Engineering, University of Mumbai)

A Thesis
Submitted to the Faculty
of the
WORCESTER POLYTECHNIC INSTITUTE
in partial fulfillment of the requirements for the
Degree of Master of Science
in
Electrical and Computer Engineering
by

January 2013

APPROVED:

Dr. Alexander M. Wyglinski, WPI, ECE, Major Advisor

Dr. Thomas Eisenbarth, WPI, ECE

Dr. Srikanth Pagadarai, ARCON Corporation

Abstract

Due to the ever increasing dependency on existing wireless technologies and the growing usage of sophisticated wireless devices, the demand for bandwidth is rising exponentially. Also, the Federal Communications Commission (FCC) has reserved a considerable amount of spectrum for licensed users. As a result, the unlicensed spectrum usage is constrained to the overcrowded unlicensed spectrum. Various spectral management surveys have indicated inefficient spectrum utilization in the licensed spectral bands. The congested unlicensed spectrum and inefficiently used licensed frequency bands calls for an approach to use the available spectrum opportunistically. Therefore, the concept of "Spectrum Pooling", which is based on Dynamic Spectrum Access (DSA), was proposed to make the unused sections of licensed spectrum available to the unlicensed users. In Spectrum Pooling, an empty section of licensed spectrum is borrowed by a secondary user for certain period of time without interfering with the licensed user.

Orthogonal Frequency Division Multiplexing (OFDM) is a transmission scheme that is a candidate for Spectrum Pooling since it is capable of forming an adaptive spectral shape that allows coexistence of licensed and unlicensed users while attemting to minimize any interference. Subcarriers in the OFDM signal can be deactivated to generate Non-Contiguous OFDM (NC-OFDM). Even though NC-OFDM allows efficient use of available spectrum, it causes out of band (OOB) radiation, which adversely affects the performance of adjacent user. This thesis presents two novel techniques for combat the effects of OOB radiation generated by NC-OFDM. The proposed techniques employ a filtering-based approach combined with the technique of windowing in order to suppress the unwanted sidelobes by around 35dB-40dB. The attenuation is achieved without affecting other transmission parameters of the secondary user significantly.

To my parents and friends

Acknowledgements

First and foremost, I would like to express my sincere gratitude to my advisor Dr. Alexander M. Wyglinski for his excellent guidance, motivation and continual support during the course of my degree. Working with him was a wonderful experience and his wide knowledge that he shared during my stay in WPI has been invaluable. He contributed significantly to both my thesis research and my professional development.

I would like to thank Dr. Thomas Eisenbarth and Dr. Srikanth Pagadarai for agreeing to be on my committee. Their suggestions and comments with regards to my thesis have helped me to improve my work. A special thanks to Dr. Srikanth Pagadarai and Harika Velamala for there continual support throughout my Master's.

During my graduate studies at WPI, I have had the pleasure of meeting many students, who have helped me directly or indirectly in completing my studies and have made my Masters a rewarding experience. I owe my thanks to them. In particular, I would like to thank WILAB members, Harika Velamala, Di Pu, Travis Collins, Zoe Fu, Le Wang, Si Chen, Sean Rocke. I also thank my close friends during my high school and under-graduation, Mayur Chipte, Ajendra Patil, Akshay Sawant, Prathamesh Kandalgaonkar, Manas Kuperkar, Hitesh Pangam, Rohan Antriwale and Tejas Mapuskar who have became an inseparable part of my life.

I am deeply indebted to my parents and my family who have been a constant source of support and love throughout this degree and my life. Thank you for everything.

Contents

List of Figures

List of Tables

List of Acronyms

AIC: Active Interference Cancellation

CC: Cancellation Carrier

CE: Constellation Expansion

CPLD: Complex Programmable Logic Deivce

CR: Cognitive Radio

DFT: Discrete Fourier Transform

DSA: Dynamic Spectrum Access

FCC: Federal Communications Commission

FFT: Fast Fourier Transform

FIR: Finite Impulse Response

FPGA: Field Programmable Gate Array

IDFT: Inverse Discrete Fourier Transform

IF: Intermediate Frequency

IFFT: Inverse Fast Fourier Transform

ISI: Intersymbol Interference

NC-OFDM: Non Contiguous - Orthogonal Frequency Division Multiplexing

OFDM: Orthogonal Frequency Division Multiplexing

OOB: Out-Of-Band

PSD:Power Spectral Density

RF: Radio Frequency

SD: Secure Digital

UHD: USRP Hardware Driver

USRP: Universal Software Radio Peripheral

Chapter 1

Introduction

1.1 Research Motivation

The demand for Radio Frequency (RF) spectrum is increasing consistently with the advent of highly sophisticated wireless technologies [5]. Growing adoption of applications that consume large amounts of available bandwidth resulting from their data-intensive content, such as online streaming music and video applications, is also responsible for the increasing demand for RF spectrum [6]. Figure 1.1 compares the demand and capacity of the spectrum over 2010-2016 in the USA [1]. It can be observed from this figure that the demand for bandwidth will exceed the bandwidth available in near future. Moreover, the governing body for telecommunications in the US, the Federal Communications Commission (FCC), has allocated a major portion of the RF spectrum to the licensed users as per the conventional spectrum allocation policies [7]. According to these policies, licensed users[1] maintain the exclusive rights to use the particular licensed frequencies in the specified geographical area. Taking

[1]In this thesis, *licensed owners* of the spectrum are also referred to as *primary users* and *legacy users*. The *unlicensed users* that use the licensed spectrum only when it is idle are refferred to as *secondary users* and *rental users*.

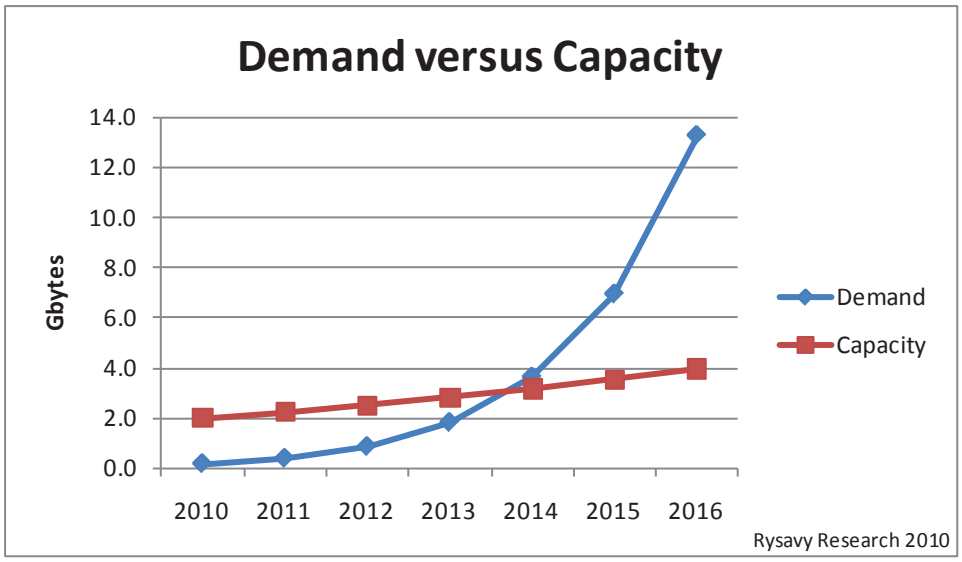

Figure 1.1: Average RF spectrum demand per user versus average RF spectrum capacity per user [1]. Notice how the demand for RF spectrum is expected to exceed the capacity sometime during 2013-2014.

unlicensed users into consideration, spectral regions, referred to as the unlicensed frequency bands, have been allocated to such users. One example of unlicensed frequency usage is the Wi-Fi Hotspots that have been installed in cafes, airports and other locations. The spectrum used for these Wi-Fi networks is mostly at 2.4 GHz and 5.2/5.3 GHz [8]. With an increasing number of secondary users, the unlicensed RF spectrum is getting overcrowded, resulting in RF interference and adversely affecting the performance of the unlicensed devices.

Furthermore, reports suggest that the licensed spectrum is not used efficiently across frequency and time [9, 10, 11]. Figure 1.2 illustrates the result of spectrum occupancy survey conducted at Worcester Polytechnic Institute, Worcester, MA, USA on July, 11, 2008 [2]. It has been observed in spectral measurements surveys that a considerable amount of spectrum is vacant, asserting that the allocated spectrum is

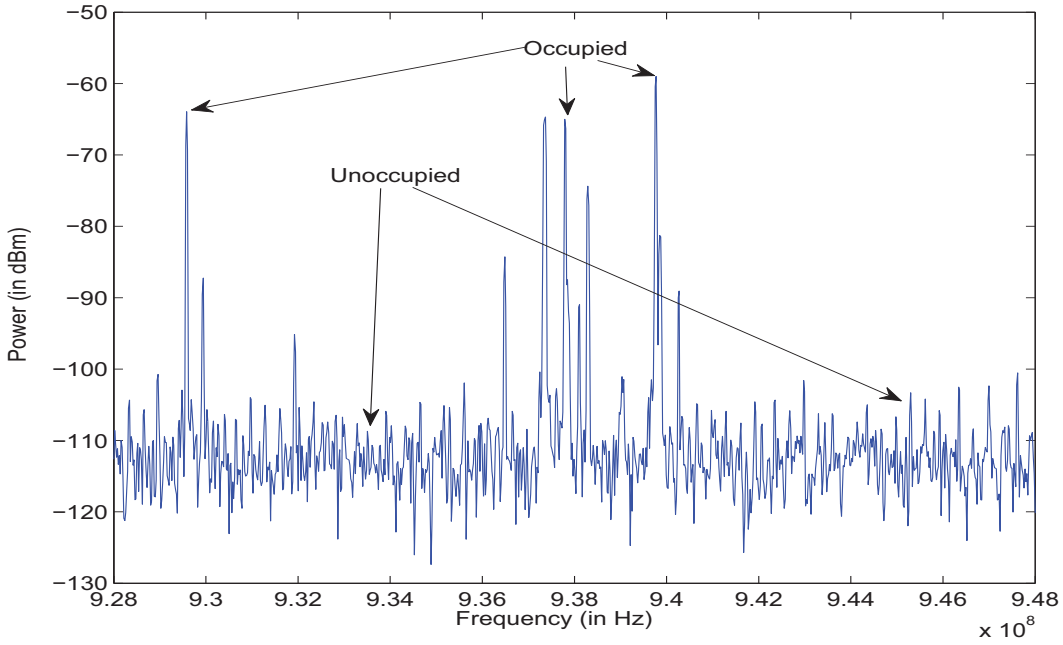

Figure 1.2: Spectrum occupancy measurements from 928 MHz to 948 MHz (7/11/2008, Worcester, MA, USA) showing that a wide section of bandwidth is vacant [2].

under-utilized. Thus, under-utilization of the licensed spectrum causes the scarcity of bandwidth. Hence, a new technology that results in efficient usage of available spectrum can be employed to solve the problem of bandwidth scarcity.

To design more efficient spectrum utilization technology, the FCC is working on the concept of Spectrum Pooling, wherein unlicensed users rent licensed sections of the spectrum from a common pool of spectral resources [12]. The term "Spectrum Pooling" was first coined in [13]. Spectrum Pooling is a technique to achieve *shared-use of primary licensed spectrum*, which is one of the various strategies of the Dynamic Spectrum Access (DSA) [14]. The other approaches of DSA as discussed in the reference [3] are *Dynamic Exclusive Use Model* and *Open Sharing Model*. As described in reference [3], DSA is a significant paradigm shift to assist RF spectral

reform, while Spectrum Pooling is a technique employed to enable DSA in order to achieve spectrum sharing between primary and secondary users. In Spectrum Pooling, the secondary user transmits across the idle portions of the licensed spectrum, thus making sure that the primary transmissions are not affected [15]. As a result of Spectrum Pooling, unlicensed users are allowed to use the spectrum that was previously inaccessible to them, while licensed users have a new source of revenue, which is generated by renting the idle spectrum to the unlicensed users [12]. Thus, Spectrum Pooling is advantegeous to the unlicensed as well as the licensed users. Also, installed hardware for the licensed system remains unchanged and perform as if there is no other system present sharing the same frequency band [12].

Figure 1.3 illustrates the concept of Spectrum Pooling, demonstrating the process of sharing the licensed spectrum. Figure 1.3(a) depicts a general spectral representation of a licensed spectrum, where vacant frequency slots are abundant. Then the secondary user starts transmitting across the idle spectrum which is shown in the Figure 1.3(b). Spectrum Pooling can be achieved in two ways, overlay system and underlay system. In an overlay system, secondary user only operates in those frequencies which are not used by primary licensed users. On the contrary, in an underlay system, secondary user uses spectrum which coincides with the spectrum of primary users resulting in minimum tolerable interference [16]. Figure 1.3(c) shows the interference that occurs since the licensed user starts using the spectrum that is being used by the secondary user. This being an overlay system, secondary user should terminate its transmission at this point to avoid the interference. Spectrum Pooling can be achieved successfully using Cognitive Radio (CR). CR is an intelligent radio that adaptively changes its transceiver parameters depending on the current spectral situation [13]. Thus, CR can be used for secondary transmission to fill the

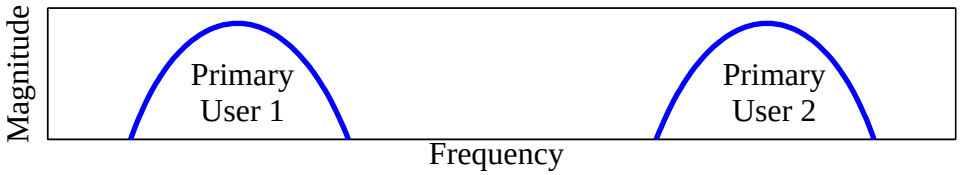

(a) Spectrum occupied only by Primary Users.

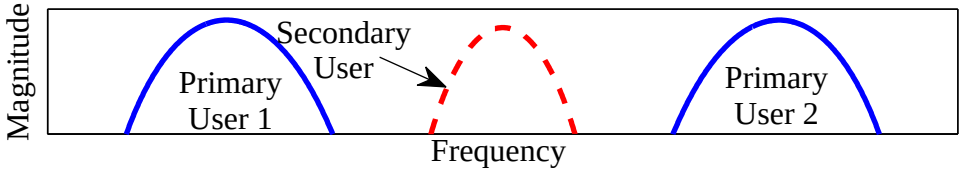

(b) Spectrum shared by Primary and Secondary Users.

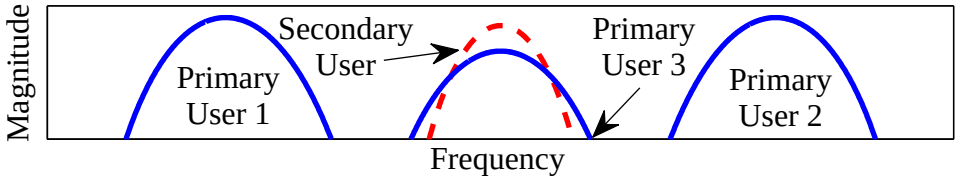

(c) Interference between Primary and Secondary Users.

Figure 1.3: Graphical illustration of "Spectrum Pooling", demonstrating the sharing of primary licensed spectrum.

spectral gaps.

Orthogonal Frequency Division Multiplexing (OFDM) is considered to be suitable for enabling Spectral Pooling because of several reasons such as, in an OFDM system, a series of bits is converted to a number of parallel data streams and each data stream is modulated with different subcarriers which are orthogonally spaced. Due to this parallelism, the symbol rate on each subcarrier is reduced, causing a decrease in sensitivity to intersymbol interference and hence a simple equalizer at the receiver [12]. Such division of spectrum into multiple orthogonal subcarriers makes the system robust to multipath channel fading. Also, a variant of OFDM, Non-Contiguous

OFDM (NC-OFDM), can be created by deactivating several subcarriers that are directly responsible for causing OOB emissions resulting in interference [17]. NC-OFDM offers a adaptive spectral shape for the secondary user that can coexist with the licensed user without any interference [18]. The advantages of using OFDM for cognitive radio-based Spectrum Pooling are the flexibility achieved by occupying the spectral gaps in the licensed bands when they are idle, deactivating the subcarriers that are coinciding with the primary user transmissions [19], the inherent frequency sub-banding [20], significantly high data rates and tolerance to multipath fading [21].

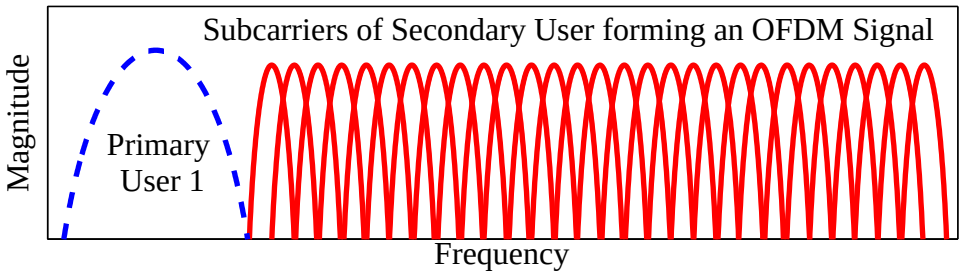

(a) Spectrum shared by Primary User and Secondary User.

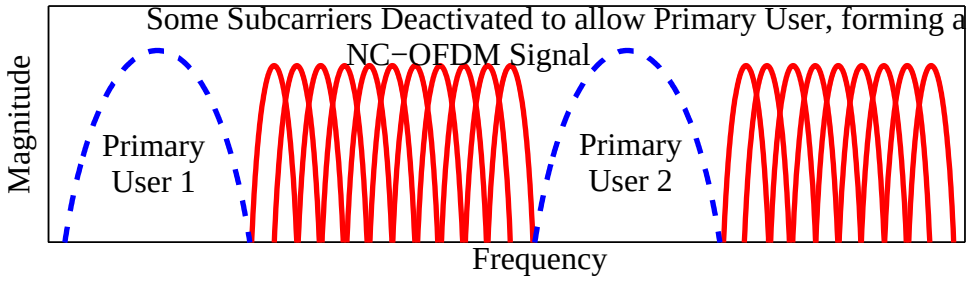

(b) Secondary User Re-adjusting itself after Primary User's Transmission Overaps it.

Figure 1.4: Schematic representation of NC-OFDM as secondary transmission for spectral pooling.

Figure 1.4 illustrates the concept of NC-OFDM used for secondary transmissions of Spectrum Pooling. Figure 1.4(a) depicts the scenario of spectrum shared between

licensed and rental users. In this scenario, if a primary user decides to transmit on the frequencies which are currently occupied by rental users, the NC-OFDM signal of the secondary user deactivates its subcarriers to accomodate the primary user. This is shown in the Figure 1.4(b).

1.2 Current State-of-the-Art

One of the key challenges in designing OFDM-based cognitive radio systems for Spectrum Pooling is considered to be the interference caused by the high sidelobe levels. These sidelobes can potentially interfere with the adjacent primary user or even the rental user transmissions. Figure 1.5 shows the high sidelobes that accompany the the single carrier waveform, which are similar to that of multicarrier OFDM waveforms. Various researchers across the world have proposed techniques to suppress these sidelobes. As specified in the reference [22], sidelobes should be suppressed to a power level of -60dB with respect to the OFDM spectrum to achieve adjacent transmissions without any interference.

As proposed in [23], sidelobe suppression can be attained by employing modulated filterbanks. Various filterbanks such as, cosine-modulated filterbanks, transmultiplexers, perfect reconstruction filterbanks, and oversampled filterbanks are discussed in this paper. Reference [24] discussed the frequency domain cancellation carrier technique for OFDM transmissions, wherein a few subcarriers with different weights are added on either side of the OFDM spectrum to negate the existing sidelobes. An adaptive optimal algorithm was proposed in [25], that tries to minimize the interference power using Mean-Square Error (MSE) solution. Reference [26] proposed a active interference cancellation (AIC) technique with reduced complexity, wherein

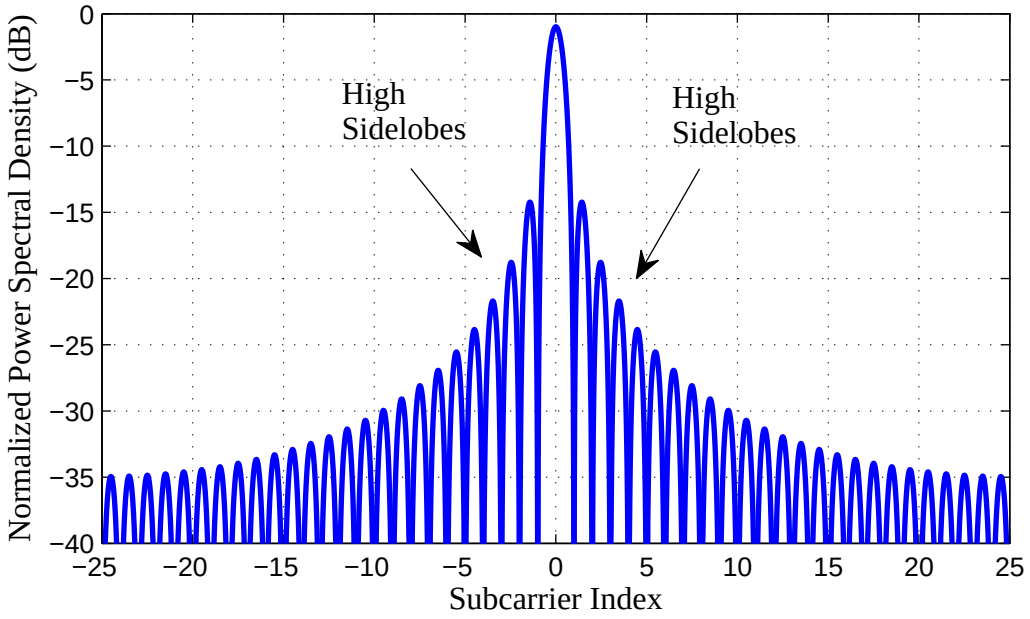

Figure 1.5: An illustration of high sidelobes accompanying a single carrier waveform. The sidelobe power level is sufficiently high to cause interference.

modulation of some subcarriers is tuned to minimize the interference caused by high sidelobes. In [27], a novel sidelobe suppression technique is proposed, wherein the input transmit symbols are paired and mapped to expanded constellations such that there is a difference of 180 degree between subcarriers in each group. Reference [28] proposed a technique to shape the OFDM spectrum using windowing and active cancellation carriers to reduce the OOB radiations. As proposed in [29], the OOB readiations of the OFDM signal are dynamically tailored to the properties of spectrum neighbors through the use of OFDM pulse shaping. A novel technique of adding extended active interference cancellation (EAIC) signals to suppress sidelobes and to shape the spectrum of the OFDM signal with a cyclic prefix was proposed in [30]. Reference [31] introduced proper carrier-by-carrier partial response signalling

between consecutive OFDM blocks to reduce OOB radiation. Recently, reference [32] proposed the combination of windowing and cancellation carrier techniques to significantly attenuate the sidelobes. Reference [32] also proposes an optimized algorithm for generation of cancellation carriers which are capable of providing a 40dB attenuation of deactivated subcarriers.

Most of the techniques mentioned here use complex algorithms and intense mathematical operations to achieve an average attenuation of 25-40dB. On the contrary, the techniques proposed in this thesis achieves an average attenuation of 35-40dB without any complex mathematical operations and with minimum changes in the primary and secondary user transmissions.

1.3 Thesis Contribution

This thesis presents two novel techniques for the suppression of sidelobes in an OFDM-based cognitive radio for dynamic spectrum access and hardware implementation of the NC-OFDM system employing the two sidelobe suppression techniques:

- **Filtering-based approach for OFDM sidelobe suppression.** The main hindrance of using an OFDM system for secondary transmissions is the high sidelobe levels. These high sidelobes causes the secondary transmissions to interfere with the licensed user and thus failing to achieve Spectrum Pooling. This thesis presents a novel filtering technique that will suppress the sidelobes sufficiently so as not to interfere with the neighboring legacy systems. A filtering based approach, which uses a Finite Impulse Response (FIR) filter, is proposed to suppress the sidelobes of the OFDM signal. A Non-Contiguous Multicarrier framework that employs filtering has been developed. Each individual FIR filter

is designed using the Least Square Linear-phase technique. The filter presents attenuation of the Out-of-band (OOB) radiation as well as of the deactivated subcarries in the case of Non-Contiguous OFDM (NC-OFDM). The suppression of around 30dB is achieved on either side of OFDM spectrum so as to reduce the amount of interference it causes to the neighboring transmissions.

- **OFDM sidelobe suppression with combined filtering and windowing.** Existing algorithms and techniques that are used for OFDM sidelobe suppression provide suppression at a cost of very complex mathematical computations at the transmitter end or at a cost of transmitting additional amount of side information to the receiver. For instance, the reference [33] uses a complex algorithm to map the present constellation to a different constellation which produces lower sidelobes. Considering the trade-off between the suppression and the complexity of the system, most of these techniques provides a sidelobe suppression of around 15dB, which is not enough for avoiding interference. This thesis provides a novel technique for OFDM suppression that will result in significant attenuation without using complex mathematical computations and any side information while transmitting. This technique is the combination of the proposed filtering method with windowing. The windowing smoothens the steep transitions on either side of OFDM spectrum, thus reducing the OOB radiation [34]. The window used in this technique is the raised cosine window since it has an advantage of having less steep edges compared to other windowing functions [34]. The roll-off factor of the raised cosine window significantly affects the performance of the system. The attenuation increases with the increase in roll-off factor. However, higher roll-off factor is also responsible for

expansion of signal duration in time domain. Hence, there is a trade-off between the attenuation achieved and the symbol duration in time domain. This technique provides the attenuation of 35dB - 40dB for a DBPSK-OFDM system with 52 subcarriers.

- **Hardware implementation of the NC-OFDM system employing filtering-based approach and windowing.** This thesis presents a hardware implementation of the NC-OFDM system emplying the proposed sidelobe techniques on the Univeral Software Radio Peripheral 2(USRP2) platform. The baseband signal is generated using Simulink and is then transmitted over-the-air using USRP2 radio. This hardware implementation and over-the-air analysis validates the performance of the proposed techniques.

Both the proposed techniques do not rely on any complex optimization techniques to provide the desired sidelobe suppressions. These techniques are independent of the number of subcarriers that are combined orthogonally to form OFDM signal. Also, these techniques do not require any modifications to be made at the receiver end in order to incorporate the changes at the transmitter. No side information is required to be transmitted along with the data carriers, thus using the transmission power efficiently. Furthermore, both the proposed techniques are validated in hardware and real-world analysis.

1.4 Thesis Organization

This thesis is organized as follows: Chapter 2 gives a brief introduction to the concepts of Dynamic Spectrum Access (DSA), Spectrum Pooling, Cognitive Radio (CR), Multicarrier Modulation (MCM), OFDM and NC-OFDM based cognitive radio for

efficient spectrum pooling. It also gives an overview of the NC-OFDM transceiver and basic OFDM generation process with an example. Universal Software-defined Radio Peripheral 2 (USRP2) platform and Simulink are also discussed in this chapter. It also addresses the problem of high sidelobes that accompany the OFDM signal. These high sidelobes are the root cause of interference between the neighboring legacy and rental users, which is the main issue of the entire thesis. Furthermore, it gives an overview of the existing techniques that are influential in attenuating these sidelobes so as to reduce the interference caused by them. In the end, it compares the existing technologies, based on the attenuation they provide. Chapter 3 discusses both the proposed sidelobe suppression techniques in detail. It also discusses the novelty of both these techniques with the concept diagrams. Chapter 4 presents the experimental setup and the experimental results obtained using the proposed techniques. It also compares both the proposed techniques with the technique proposed in the reference [2]. Finally, chapter 5 draws several conclusions and presents the directions for future work.

Chapter 2

NC-OFDM-based Cognitive Radio Transmission

This chapter provides an introduction to the Spectrum Pooling-based cognitive radio. It also gives an overview of Orthogonal Frequency Division Multiplexing (OFDM). The implementation of Non-Contiguous OFDM (NC-OFDM) system for secondary transmissions of spectrum pooling is described with an example. It also discusses the use of Universal Software-Defined Radio Peripheral 2 (USRP2) platform as cognitive radio and Simulink as an interface to communicate with USRP2 through a computer. Furthermore, it addressses the issue of high Out-of-Band (OOB) Radiation in an OFDM signal and several existing techniques to suppress these radiations.

2.1 An Overview of Cognitive Radio System for Spectrum Pooling

As discussed in [12], wireless applications are getting more sophisticated and are being used widely, causing a substantial increase in demand for the bandwidth. Ref-

erence [9] has shown that the current spectrum allocation techniques are inefficient in making the full use of available spectrum. The Federal Communications Commission's (FCC's) spectrum allocation policies are based on traditional techniques, where a section of spectrum is allocated to a particular user for a particular geographical area. In an observation made by the FCC in [35], due to the static allocation of spectrum to the users, the licensed spectrum is heavily underutilized across a particular frequency and time. As a result, they determined that it was time for a new technique that would be capable of intelligently allocating the spectrum among several users in such a way that the available frequencies will be used more efficiently. This new technology was called Dynamic Spectrum Access (DSA) [2].

2.1.1 Dynamic Spectrum Access (DSA)

Dynamic Spectrum Access (DSA) is an emerging wireless communication paradigm. The primary aspect of DSA systems is their ability to use knowledge of their electromagnetic environment to adapt their operation and access in order to spectrum [36]. The key promise of these systems is that they open up the possibility of highly flexible and efficient management of spectrum. As illustrated in the Figure 2.1, DSA strategies can be broadly categorized under three models.

- *Dynamic Exclusive Use Model*: The main idea of this model is to introduce flexibility to improve spectrum efficiency. Two approaches have been proposed under this model: Spectrum property rights, and Dynamic spectrum allocation. The former approach allows license holders to sell and trade spectrum and to freely choose technology. On the contrary, in the second approach, spectrum is allocated to services for exclusive use in a given region and at a given time.

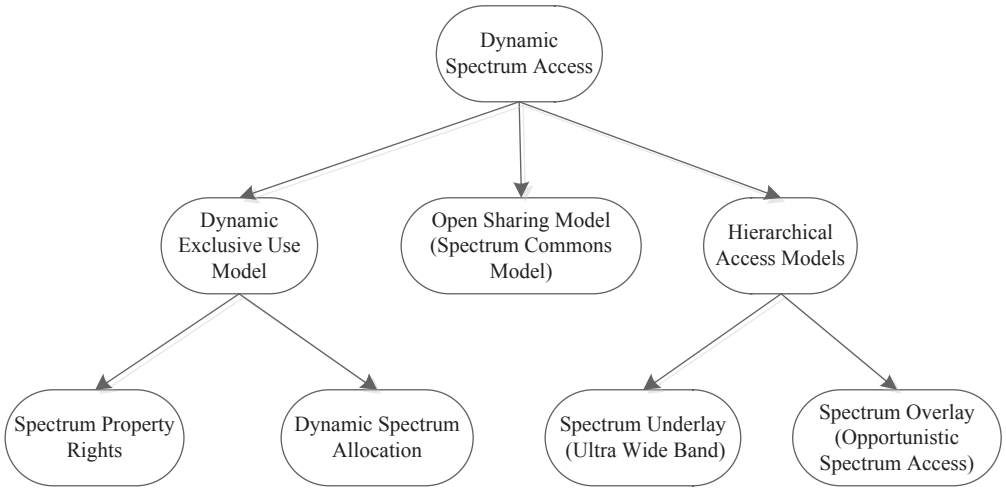

Figure 2.1: A taxonomy of the dynamic spectrum access [3], showing various DSA techniques.

- *Open Sharing Model*: This model employs open sharing among peer users as the basis for managing a spectral region [3], where all the peers have equal rights to access the shared spectrum.

- *Hierarchial Access Model*: The basic idea of this model is to allow secondary users to access licensed frequency while limiting the interference with primary users. Two approaches to spectrum sharing between primary and secondary users have been considered: Spectrum Underlay and Spectrum Overlay. In a Spectrum Underlay system, secondary user uses spectrum which coincides with the spectrum of primary users resulting in minimum tolerable interference [16]. In an overlay system, secondary user only operates in those frequencies which are not used by primary licensed users. Spectrum Overlay was first defined in reference [13] under the term spectrum pooling. Spectrum Pooling is a spectrum management principle whereby primary users put their unused spectrum into

a virtual pool from which secondary users can rent spectrum.

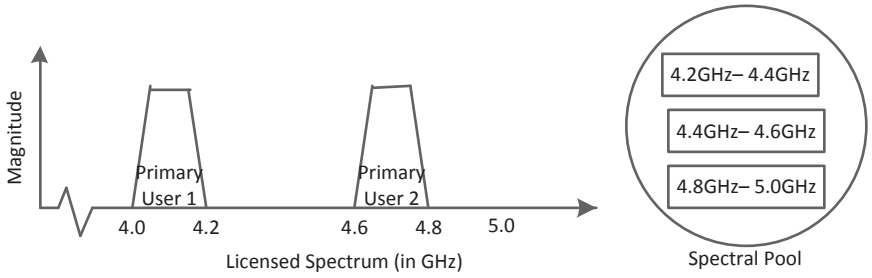

(a) Licensed Spectrum with two Primary Users.

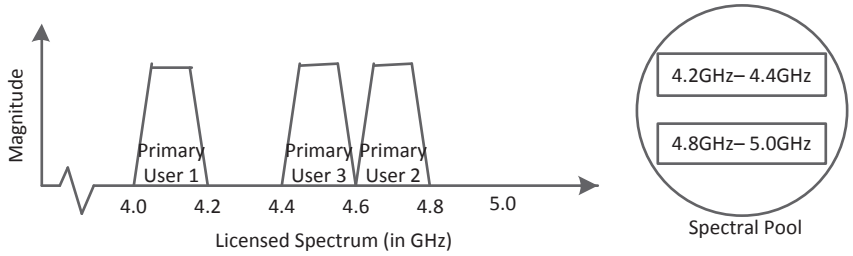

(b) Licensed Spectrum with three Primary Users.

Figure 2.2: An illustration of the concept of "Spectral Pooling" showing the borrowing of the spectrum from the pool.

Figure 2.2 shows the concept of virtual pool that stores the available spectral ranges. In this figure, it is considered that the spectral range allocated to the primary user is 4GHz to 5GHz. As shown in Figure 2.2(a), primary users occupies the range 4GHz to 4.2GHz and 4.6GHz to 4.8GHz. Thus, the spectral ranges 4.2GHz to 4.6GHz and 4.8GHz to 5GHz are allocated to the spectral pool. Figure 2.2(b) is a continuation of the scenario shown in Figure 2.2(a), where an additional primary user starts transmitting on the spectral range 4.4GHz to 4.6GHz. As a result, the spectrum in the pool is reduced. A secondary user is allowed to temporarily rent these frequncies from this pool. As discussed in [12], Spectrum Pooling can be achieved

without any modifications in the primary user devices. Furthermore, the licensed system can function as if there is no other devices using the same spectral range. Even though Spectral Pooling can be an additional source of income for the licensed user, there are several technological, political, legal and economic problems arising from the implementation of this system. However, once the technical obstacles are overcome and the feasibility of Spectrum Pooling is proven, politics cannot refuse this idea [12]. The economic problems can be solved by involving both industrialists and research institutions in the implementation of these systems.

2.1.2 Cognitive Radio (CR)

Flexible spectrum pooling is made possible by Cognitive Radio (CR) technology, which is an extension of Software Defined Radio (SDR) technology, where the wireless platform rapidly configures its parameters depending upon the current spectral usage and environment [37]. CR is an autonomous unit that intelligently configures its transceiver parameters depending on the environment and the present spectral usage scenario so as to transmit within the spectral gaps [13]. As a result, this process enables the secondary utilization of the licensed spectrum.

Figure 2.3 shows the concept diagram of Cognitive Radio (CR). CR has a SDR, featuring as a radio environment. A CR senses the spectrum using SDR, analyses the spectrum and finally changes its transceiver parameters accordingly. An important issue in achieving efficient DSA is detecting a idle spectral range and transmitting in that spectral gap without interfering with the neighboring transmissions. This can be achieved with the help of Software Defined Radio (SDR).

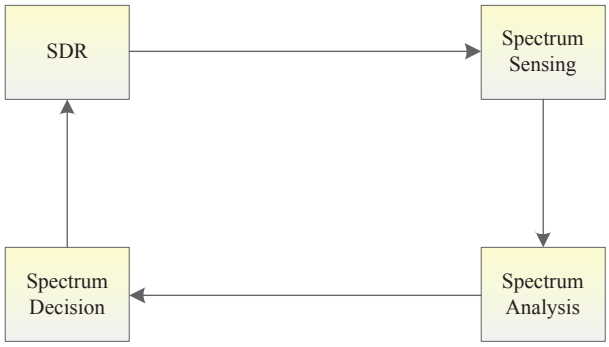

Figure 2.3: A concept diagram of cognitive radio (CR) showing the basic procedure performed by CR.

2.1.3 Software Defined Radio (SDR)

In a conventional radio, various communication subsystems such as filters, modulators, demodulators, and amplifiers are implemented in hardware. As a result, it fails to provide any flexibility. Conversely, Software Defined Radio (SDR) is a radio communication system where the communication subsystems are implemented by means of software on a computer or an embedded system [38]. A SDR usually consists of a processor, an Analog-to-Digital Converter (ADC), a Digital-to-Analog Converter (DAC) and a RF front end. Based on the same hardware, different transmitter/receiver algorithms are implemented in software [39]. Thus, SDR provides a large amount of flexibility compared to the conventional radio. The term "Software Radio" was coined in 1985 by a team at the Garland Texas Division of E-Systems [40]. The Software Radio described in this article had digitally matched filters that automatically adapted to the characteristics of the incoming signal environment to demodulate complex signals corrupted by interference [40]. In 1995, U.S. military undertook a project named SpeakEasy, whose primary goal was to

use programmable processing to emulate more than 15 existing military radios [41]. Software reprogammability of waveform is the key aspect of SpeakEasy which is achieved by the programmabale Digital Signal Processors (DSPs). Over the years, several SDRs have been introduced in the market.

Table 2.1: Comparison chart of commonly used SDR platforms.

Name	Frequency range	Sampling Rate	Connection	Base Price
ADT-200A [42]	10 kHz - 30 MHz	-	USB, Internet Remote	$5447
AOR AR-2300 [43]	40 kHz - 3.15 GHz	65 MSPS	USB	$3,299
Elad FDM-S1 [44]	20 kHz - 30 MHz	61.44 MHz	USB	$549
Elecraft KX3 [45]	0.5 - 54 MHz	-	USB	$900
FLEX-5000A [46]	0.01 - 65 MHz	48, 96, 192 kHz	1394a Firewire	$2,800
Matchstiq [47]	300 MHz - 3.8 GHz	40 MSPS	USB	$4,500
Perseus [48]	10 kHz - 40 MHz	80 MSPS	USB	$1,199
Mercury [49]	0.1 - 55 MHz	123 MSPS	USB	$469
USRP2 [50]	Up to 4 GHz	100 MSPS	Gigabit Ethernet	$1,500
WR-G31DCC [51]	9 kHz - 50 MHz	100 MSPS	USB	$950
NetSDR [52]	0.1 kHz - 34 MHz	80.0 MHz	Ethernet	$1,450

Table 2.1 lists the several commonly used SDR platforms with their primary features. Considering the trade-off between the operable frequency range, sampling rate and the price, Universal Software-defined Radio Peripheral 2 (USRP2) comes out to be the most appropriate choice. Also, the on-board Gigabit Ethernet Interface allows the applications to send as high as 50MHz of RF bandwidth in and out of the USRP2. Hence, USRP2 is used as a radio platform in this thesis.

2.1.4 Universal Software Radio Peripheral 2 (USRP2)

The Universal Software Radio Peripheral (USRP) family of products has been developed by Matt Ettus of Ettus Research LLC [53]. The company entered the

field of software defined radio with their first product, the USRP. The advanced version, USRP2, was made available for limited number of developers in September 2008 [54]. However, USRP2 was officially released in May 2009 and has been followed by several successive products.

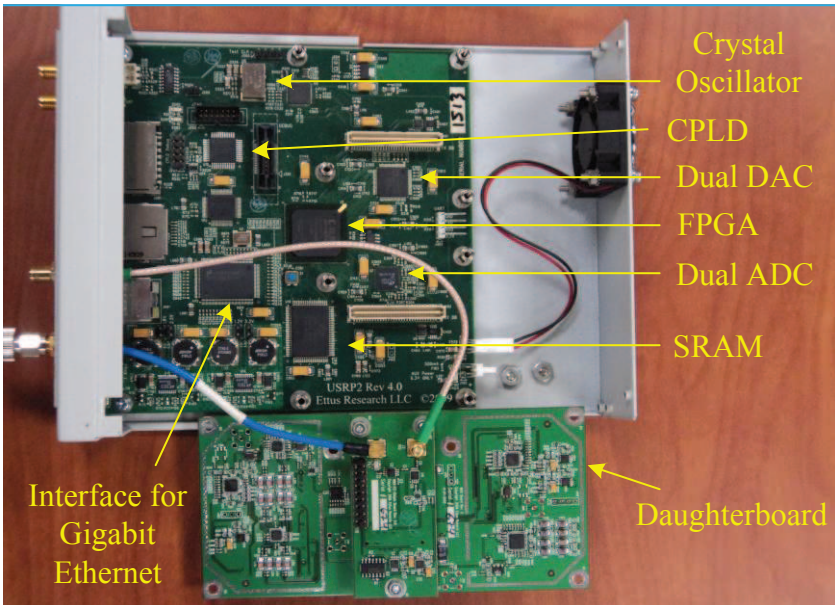

Figure 2.4: Photograph of the USRP2 SDR platform showing its major components.

Figure 2.4 shows a photograph of the USRP2. The USRP2 is a versatile software defined radio platform consisting of a motherboard and a daughterboard. The motherboard has a Xilinx Spartan XC3S2000 FPGA installed on it that provides high sample rate processing. The two 100 Mhz, 14-bit ADC and two 400 Mhz, 16-bit DAC allow for the wider band signal and an increase in dynamic range at the same time. The daughterboard has an analog circuitry that upconverts the signal at Intermediate Frequency (IF) to passband frequency. There are various types of daughterboards available in market, each of which provide a different specification

Table 2.2: Comparison chart of commonly used daughterboards for USRP2 platform.

Model	Frequencies Supported	Type	Transmit Power (mW)
Basic Tx	1 MHz - 250 MHz	2 Tx	100
Basic Rx	1 MHz - 250 MHz	2 Rx	100
WBX	50 MHz - 2.2 GHz	Tx/Rx, Full-Duplex	100
SBX	400 MHz - 4.4 GHz	Tx/Rx, Full-Duplex	100
XCVR	2.4 GHz to 2.9 GHz 4.9GHz to 5.9 GHz	Tx/Rx, Half-Duplex	100

to the USRP2. Table 2.2 compares the most commonly used daughterboards for USRP2 [53].

Figure 2.5 depicts the general schematic of the USRP2. As shown in the figure, the USRP2 has an on-board Gigabit Ethernet interface that allows the applications to send 50MHz of RF bandwidth in and out of the USRP2. Configurations and

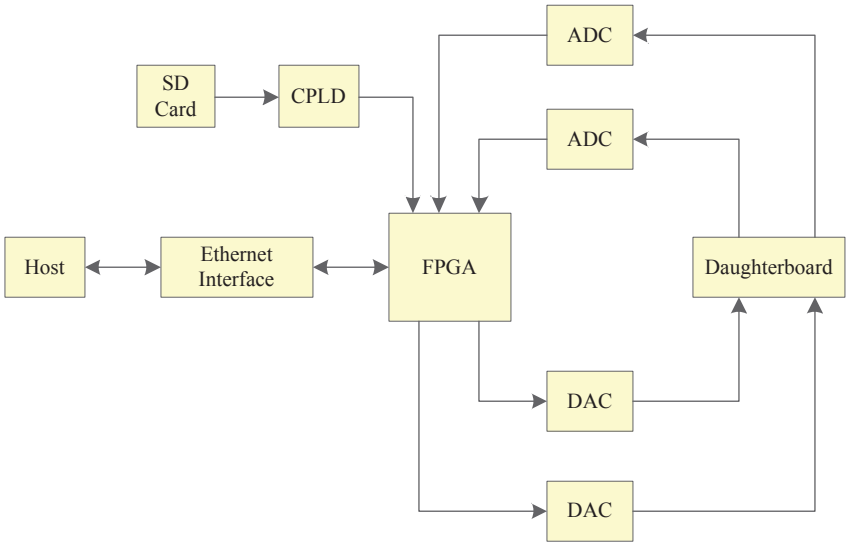

Figure 2.5: General schematic of the USRP2 showing the internal datapath.

firmware required by USRP2 are stored in a Secure Digital (SD) card which allows

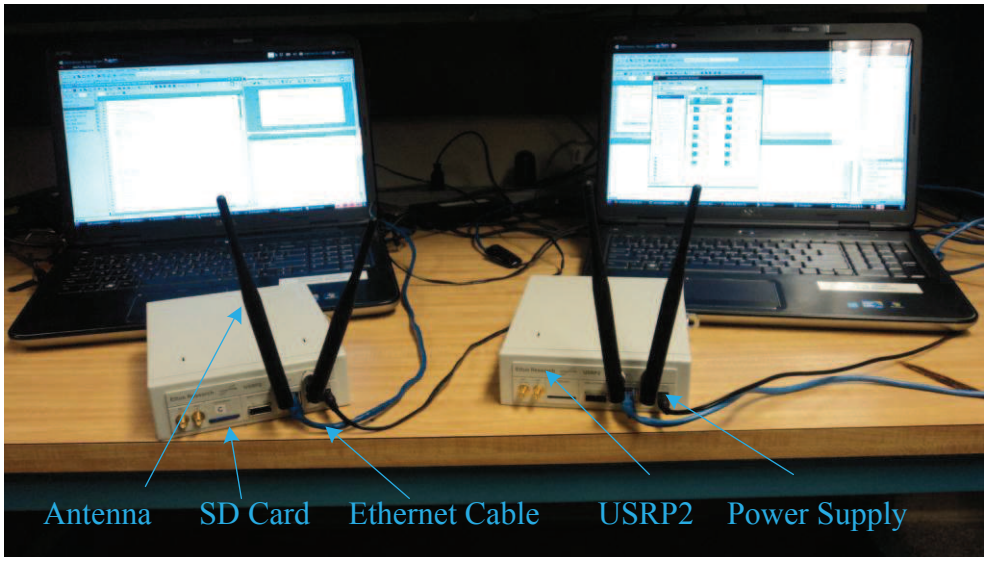

Figure 2.6: Experimental setup demonstrating the use of USRP2 platform for wireless communication.

easy programming without special hardware. The on-board Complex Programmable Logic Device (CPLD) loads the bit file from the SD card onto the FPGA when the USRP2 is turned on. CPLD enters a pass through mode once the bit file is loaded, which enables the FPGA to access data on the SD card. USRP2 has an inbuilt high speed SRAM with a memory of 1 Megabyte. It also has digital downconverters with programmable decimation rates and digital upconverters with programmable interpolation rates, which helps in controlling the sampling rate.

Figure 2.6 shows a general experimental setup of wireless communcation on a USRP2 platform. The figure shows all the major user-controlled sections required for using USRP2. The USRP2s shown in this figure are using XCVR daughtercards and hence are capable of providing half-duplex communication. Of the two USRP's shown, one acts as a transmitter while other acts as a receiver. The Ethernet cable serves as a high speed connection between the USRP2 and the host, which is the

laptop in this case. For the USRP2, acting as a transmitter, input through the ethernet cable is a signal at baseband frequency. The USRP2 translates the input signal into radio frequency (RF) and transmits it over-the-air using the antennas shown. The reverse process is followed at the receiver. The USRP2 acting as the receiver, absorbs the transmitted signal in the form of elctromagnetic radiations, using the antennas. The recevied RF is converted to baseband in the USRP2. Finally, the baseband signal is transported to the host, *e.g.* laptop, through the ethernet cable.

2.1.5 Interfaces to Control the USRP2 platform

The USRP hardware driver (UHD) is the device driver developed by the Ettus Research for use with the USRP family [55]. It works with all major operating systems such as Linux, Mac and Windows. The goal of UHD is to provide a host driver and an Application Programming Interface (API) for current and future Ettus Research products. Several software frameworks including GNU Radio and Simulink use UHD.

GNU Radio is an open source toolkit that provide signal processing algorithms for implementing SDR prototypes. GNU Radio applications are primarily written using the Python programming language, while the performance-critical signal processing path is implemented in C++. GNU Radio also provides a GNU Radio Companion which is a graphical programming environment. Even though GNU Radio enables the use of very high sampling rates, it is a very complex tool to control USRP2. On the other hand, the MathWorks provide plug-ins which are easy to install and creates the interface between Simulink and USRP2. These plug-ins facilitate the control over USRP2. Hence, we will be using Simulink as an interface between the

computer and the USRP2 in this thesis.

2.1.6 An Overview of Simulink

Simulink is a powerful tool that serves as an interface between the USRP2 and the computer which is acting as the host. Simulink, developed by MathWorks, is an interactive graphical environment for model-based designs and simulations. It has a set of customizable block libraries that allows users to design, simulate and test a variety of systems, that includes communication and signal processing [56]. MATLAB and Simulink connect to USRP2 to provide a radio-in-the-loop design and modeling environment. The research work presented in this thesis makes extensive use of Simulink.

Figure 2.7 illustrates a general usage of Simulink as a graphical tool to generate and plot any desired signal. Figure 2.7(a) shows a Simulink model, `siggen.mdl`, that is running and a scope which continuously shows the output of the model in frequency domain. The model `siggen.mdl` is simply a Simulink implementation of the sine wave generator. Figure 2.7(b) shows the spectrum scope displaying the frequency response of the output signal. It makes use of several Simulink blocks which are pre-defined and located in the Simulink library. Simulink Library consists of a wide variety of in-built blocks such as modulators/demodulators, multiplexers/demultiplexers, and logic gates. Figure 2.8 shows the screenshot of the Simulink Library Browser. The built-in blocks can be simply *dragged and dropped* into the Simulink model. The block properties can then be changed to match the desired functionality. The screenshot in Figure 2.7 also shows various other vital features provided by Simulink. The dimensions of the signal, output from each block, are shown immediately after the block in the form "[358x1]". The color of the block

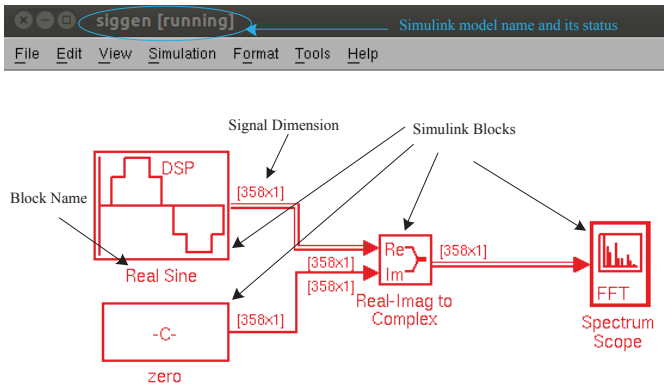

(a) Screenshot of a Simulink model.

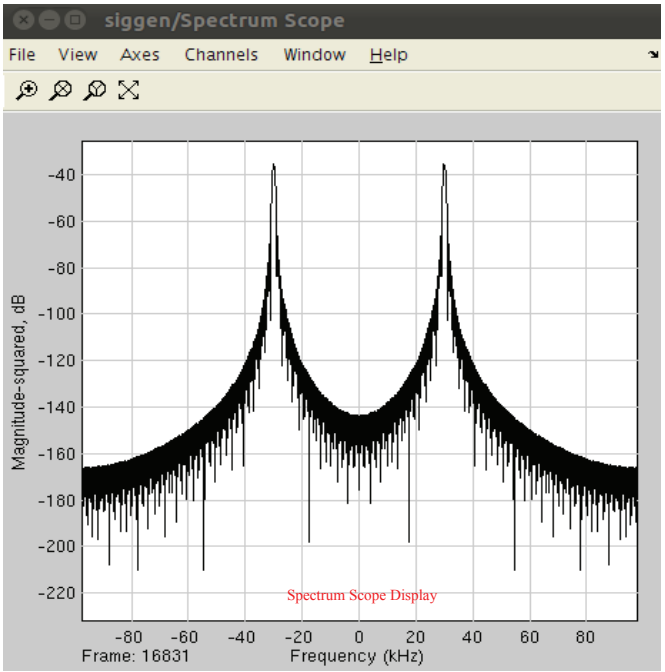

(b) Screenshot of the Spectrum Scope showing the output signal.

Figure 2.7: A screenshot demonstrating the use of simulink for generating and plotting a frequency response of a sine wave.

signifies the sample rate of the signal output from that block. In other words, the blocks with same color code are outputting the signals with same sampling rates.

The format-specifiers such as the signal dimensions and the sampling rates are very useful in understanding the signal operations as well as in debugging the model if something is not working properly.

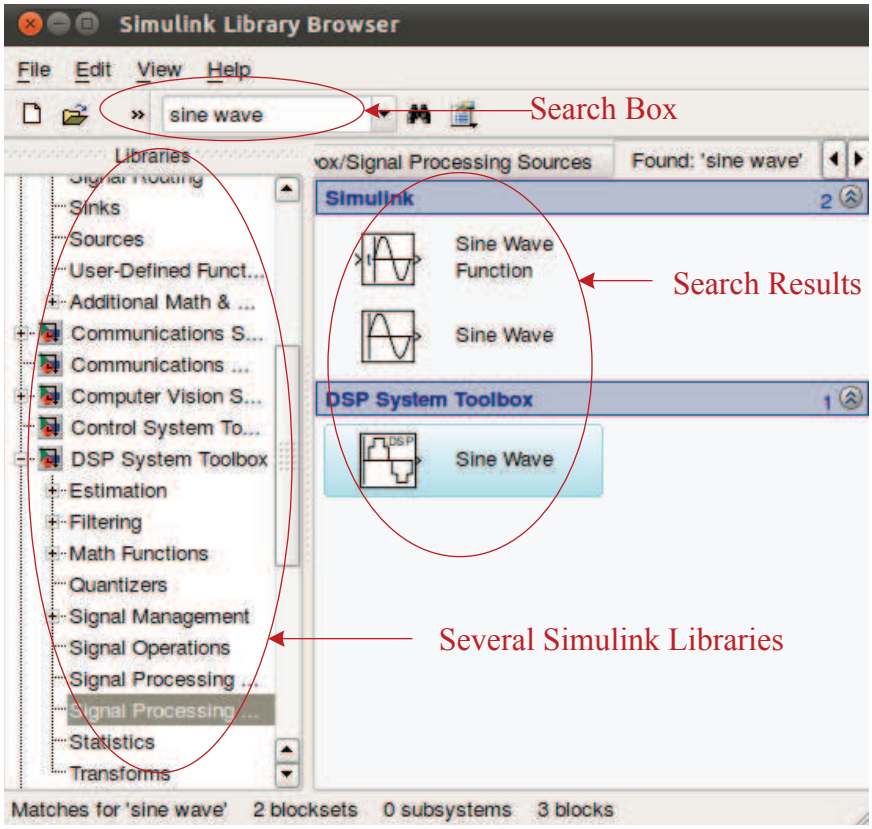

Figure 2.8: A screenshot of Simulink Library Browser showing the search results for "Sine Wave".

As discussed in the previous subsection, the MathWorks provides plug-ins that enables Simulink to act as an interface between the USRP2 and the host, such as a laptop. The Simulink has a built-in block, the SDRu Transmitter, which is responsible for conversion of the input baseband signal to passband signal, which is ultimately given to the USRP2 through the ethernet cable for over-the-air trans-

mission. The counterpart of this block also exists and is referred to as the SDRu Receiver. It is responsible for conversion of passband frequency from USRP2 receiver to the baseband frequency, making it operable for Simulink. Figure 2.9 shows the screen capture of the "SDRu Transmitter" and the block properties of the same. As shown in the Figure 2.9, the block proerties of "SDRu Transmitter" shows two types of properties:

- *User controlled properties* such as center frequency, gain and interpolation factor
- *Hardware properties* such as type of the daughterboard installed and operable frequency range.

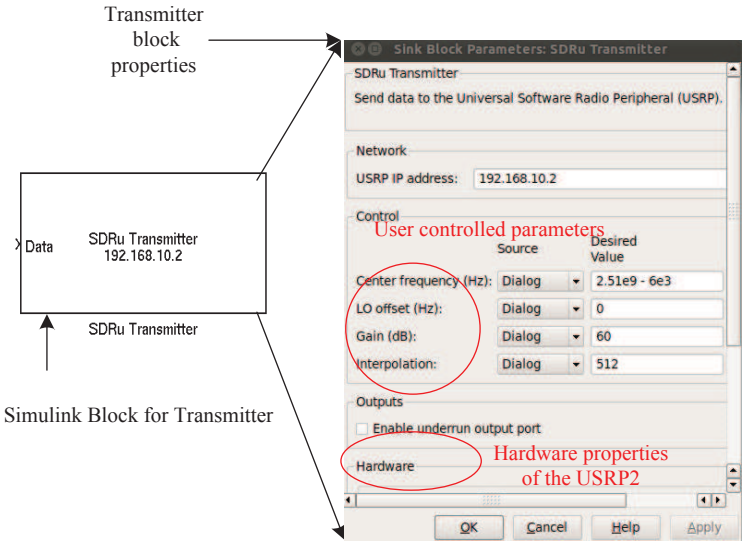

Figure 2.9: A screenshot of the "SDRu Transmitter" block and its block properties.

SDRu Receiver does the exact reverse operation. Unlike SDRu Transmitter, it has one output port and no input port. Furthermore, the user controlled properties

of SDRu Receiver includes “Decimation Factor” instead of “Interpolation Factor”.

As this section discussed all the tools that will be used in this thesis as well as the vital topics like CR, DSA, SDR and USRP2, the next section deals with Orthogonal Frequency Division Multiplexing (OFDM) and Non Contiguous OFDM (NC-OFDM).

2.2 Orthogonal Frequency Division Multiplexing (OFDM)

Dynamic spectrum access (DSA) is the novel approach that enables highly flexible and efficient management of spectrum. The primary aspect of DSA systems is their ability to use knowledge of their electromagnetic environment to adapt their transmissions and access the spectrum without interfering neighboring transmissions [36]. A possible transmission technique for realizing DSA is Orthogonal Frequency Division Multiplexing (OFDM) [57], a multicarrier modulation scheme based on data parallelism that is achieved by dividing a high speed bit stream into several slow bit streams and modulating each of them with subcarriers which are orthogonal to each other. By leaving a set of subcarriers unused, OFDM provides a flexible spectral shape that fills the spectral gaps without interfering with the primary users [58].

2.2.1 An Overview of Multicarrier Transmission

In a single-carrier modulation such as Amplitude Modulation (AM) or Frequency Modulation (FM), the input bit stream is modulated by just one carrier wave. Conversely, in a multi-carrier modulation scheme, a single bit stream is parsed into several slower bit streams. These slower bit streams are modulated by different carrier frequencies which are also called as subcarriers. The modulated data from each

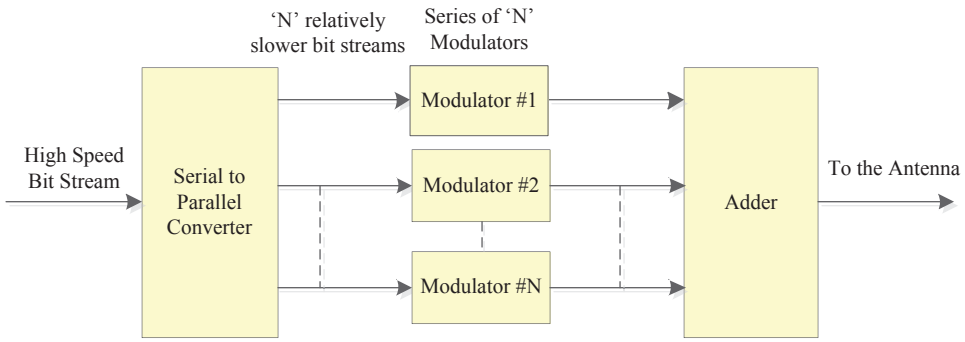

Figure 2.10: General schematic representation of Multicarrier Transmission.

subcarrier is then added together prior to the transmission [59].

Figure 2.10 depicts the general schematic representation of a multi-carrier transmission. As shown in the Figure 2.10, a high speed bit stream is divided into "N" slower bit streams. These parallel bit streams are given as an input to "N" different modulators and the modulated signals are added together prior to the transmission.

Figure 2.11 compares the single carrier wave and multi-carrier waves in frequency domain. As shown in the Figure 2.11, each of the subcarrier uses a narrow bandwidth compared to the wideband used by the single carrier. However, the bandwidth of the composite signal formed by the subcarriers may be wide. The subcarriers are placed Δf apart from each other across any available frequency band [60].

Figure 2.12 shows the comparison of single carrier wave and multi-carrier waves in time domain. It can be seen from the Figure 2.12 that the time period of the subcarrier is less than the previous subcarrier by a factor of Δt, where $\Delta t = 1/(\Delta f)$.

Multicarrier modulation is a type of Frequency Division Multiplexing (FDM) [60]. In a traditional FDM scheme, the available bandwidth is divided into a series of non-

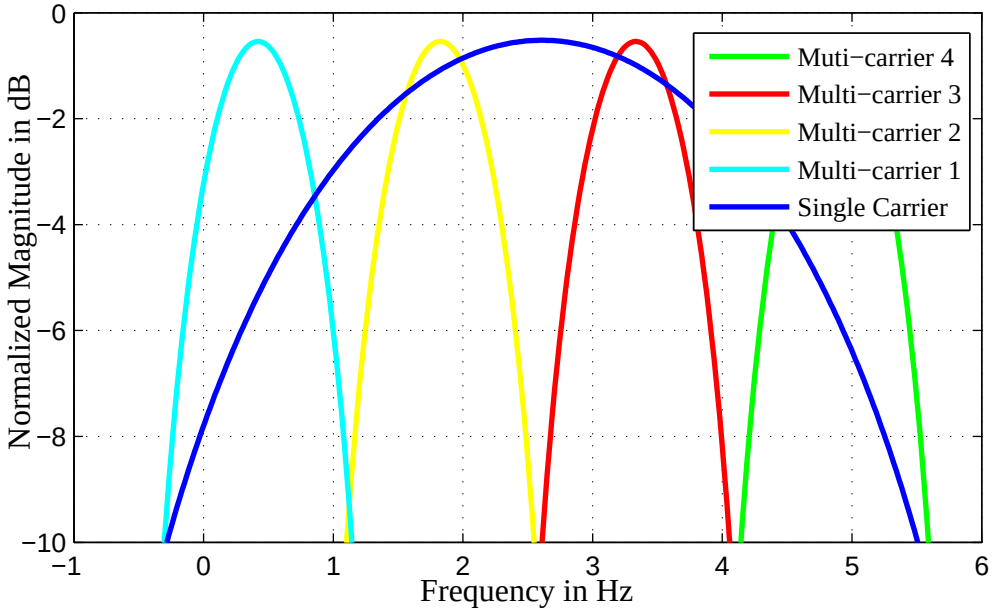

Figure 2.11: An illustration of single carrier wave and multi-carrier waves in frequency-domain.

overlapping sub-bands which are used as carrier frequencies [4]. If modulated this way, it is straightforward to filter out the required carrier signals and demodulate them at the receiver since there are guard bands placed between two adjacent carriers. This technique has spectral gaps functioning as guard bands, resulting in inefficient usage of spectrum. Referring to Figure 2.13, the available bandwidth is divided into four distinct carrier frequencies, namely f_1, f_2, f_3 and f_4.

However, it is possible to make the carrier frequencies overlap each other and still demodulate it correctly if the carrier frequencies can be made to be orthogonal. To make the carriers orthogonal,

following condition should be satisfied [61]:

$$\int_0^T \sin(2\pi f_m t) * \sin(2\pi f_n t)\, \mathrm{d}t = 0. \tag{2.1}$$

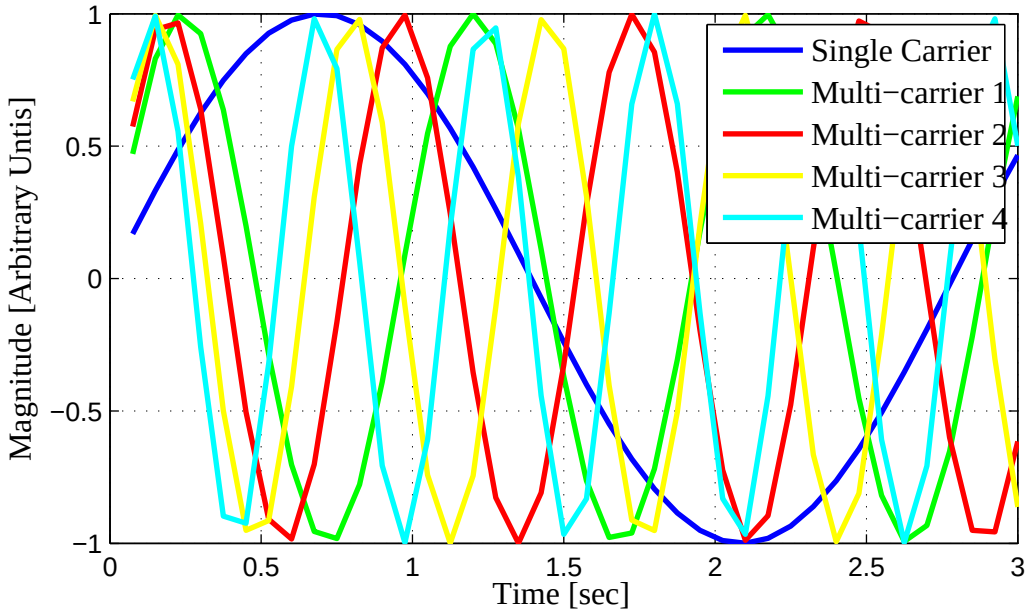

Figure 2.12: An illustration of single carrier wave and multi-carrier waves in time-domain.

where, the two sine functions represents two carrier waves with frequencies f_m and f_n and T being the time period. Equation (2.1) can be solved and simplified further to the form:

$$f_m - f_n = \frac{N}{2T}, \qquad N = 1, 2, 3, 4..... \tag{2.2}$$

If modulated orthogonally, data can be decoded correctly despite overlapping one another.

2.2.2 A General Schematic of an OFDM based Cognitive Radio Transceiver

This subsection explains the fundamentals of generating a OFDM signal using a general schematic of the entire transceiver system. Figure 2.14 depicts the general schematic of the OFDM transmitter. Let the input to the transmitter be a high

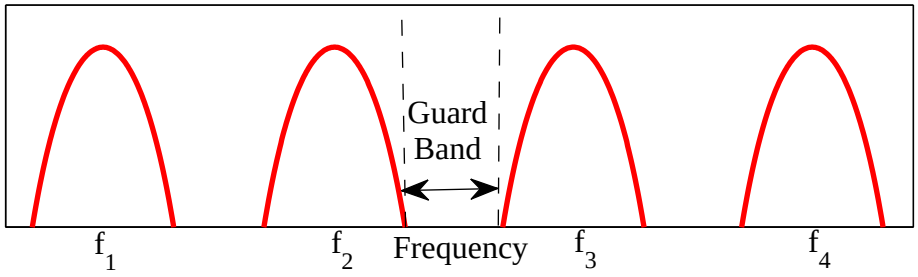

(a) Conventional FDM.

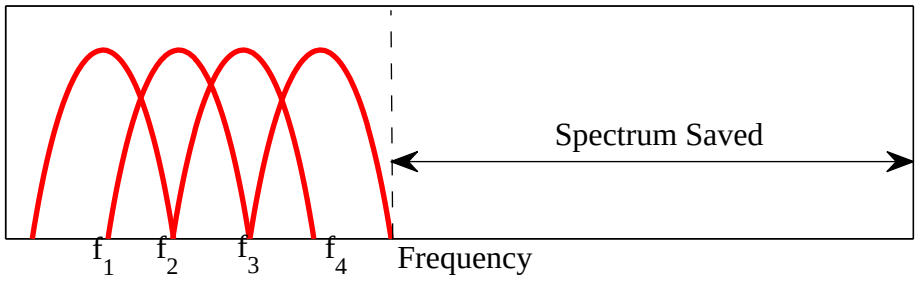

(b) Orthogonal FDM.

Figure 2.13: Graphical illustration of the difference between Conventional and Orthogonal FDM [4].

speed binary data stream:

$$d = [d_0, d_1, ..., d_{n-1}]. \tag{2.3}$$

This stream of data then goes through a Modulator giving the symbols as output. Let those symbols be

$$x = [x_0, x_1, ..., x_{n-1}]. \tag{2.4}$$

This stream of modulated data is then split into N slower data streams using a Serial-to-Parallel (S/P) Converter, where N defines the number of sub-carriers. Each of the slower data stream x_i, where i = *0,1,2,....,N-1*, is modulated by a different subcarrier in such a way that all the subcarriers are orthogonal to each other. This can be achieved by performing an *Inverse Discrete Fourier Transform (IDFT)* on

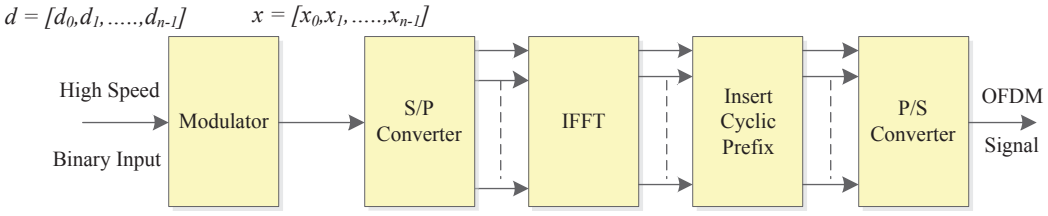

Figure 2.14: General schematic representation of OFDM Transmitter.

the parallel data stream as proposed in [62] by Weinstein and Ebert. In the block diagram shown in Figure 2.14, Inverse Fast Fourier Transform (IFFT) is used, which is an efficient way of performing IDFT. The modulated data from each subcarrier is then added together to obtain a composite OFDM signal.

The high data rate is the primary cause of Inter-symbol Interference (ISI). Increase in data rate decreases the time duration and as a result of this, self interference due to the multipath delay spread occurs. To avoid this problem, guard band is prepended to the data such that ISI occurs in the guard interval which can be removed at the receiver and the data can be retrieved. The most effective guard interval to use is a cyclic prefix of the symbol [63, 64]. Cyclic prefix will effectively extend the length of the symbol without altering the frequency of the carrier wave as shown in Figure 2.15. Figure 2.15 shows four subcarriers with a cyclic prefix which is nothing but the end of the signal prepended to itself. Hence, the frequency of the carrier wave remains unchanged and owing to this, the orthogonality of the OFDM signal is preserved. Cyclic prefix acts as a buffer region where delayed information from the previous symbols can get stored. Hence, the length of the cyclic prefix is selected such that it is greater than the channel spread. The receiver has to exclude samples from the cyclic prefix which got corrupted by the previous symbol when choosing the samples

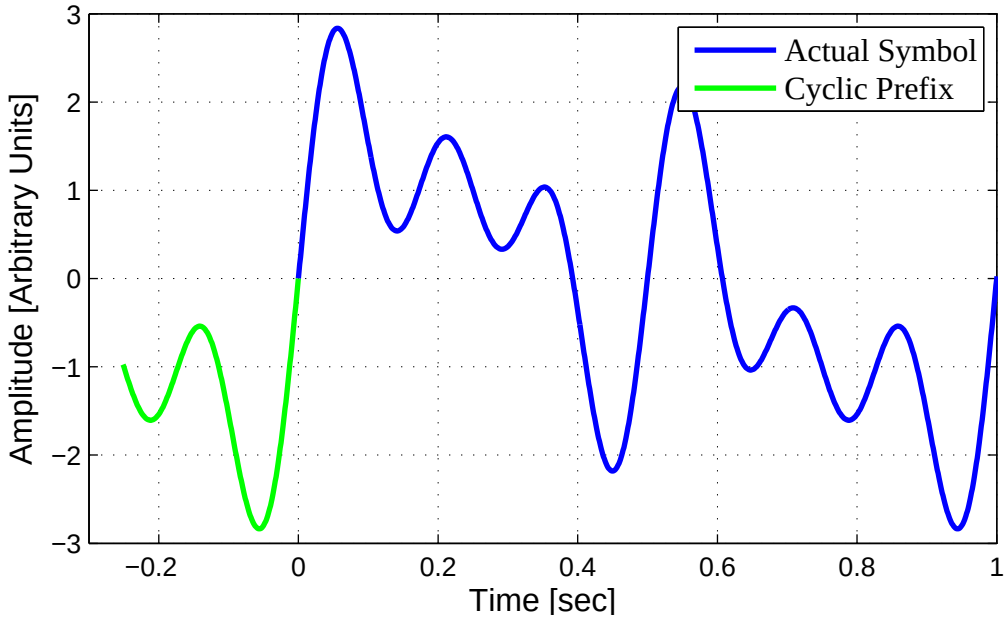

Figure 2.15: An illustration of attaching cyclic prefix to four subcarriers.

for an OFDM symbol [63].

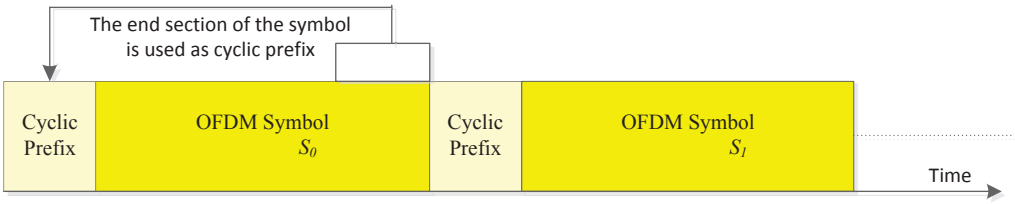

Figure 2.16: An illustration of insertion of the cyclic prefix.

Figure 2.16 shows the procedure of insertion of cyclic prefix graphically. The tail section of the OFDM symbol is used as the prefix so that the frequency of the symbol remains unaltered. As shown in the Figure 2.14, the serial signal is converted to parallel form using parallel to serial (P/S) converter, just before the transmission.

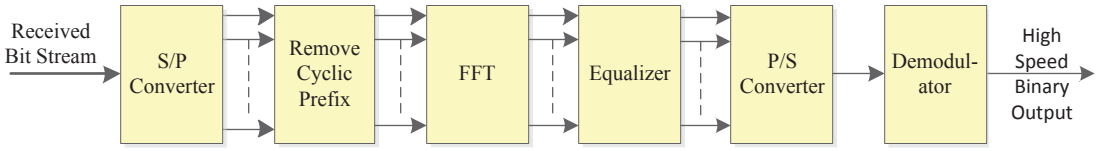

Figure 2.17: General schematic representation of OFDM Receiver.

Figure 2.17 depicts the general schematic of the OFDM receiver. It does the reverse operation of what is being done at the transmitter. Received serial bit stream is converted to parallel streams using S/P converter. The cyclic prefix is then removed from each of the parallel data stream to get the modulated subcarriers. Demodulation is then achieved by performing Discrete Fourier Transform (DFT) [62]. The cyclic prefix in the OFDM prevents the intersymbol interference. However, intrasymbol interference still persists because of the signal interfering itself and the amplitude and phase of each sub carrier is corrupted as a result of it. To mitigate these effects, multipath channel behavior is estimated with the help of some reference subcarriers. Therefore, having the estimated behavior of the channel, the equalization can be performed by several equalizers composed by a single tap at each frequency of the received signal [65]. After performing equalization and P/S conversion, demodulation is performed to recover the original high speed binary data stream.

2.2.3 An Example Demonstrating the OFDM Signal Generation

Let us work through the process of OFDM signal generation via an example. Let the high speed input be:

$$d = [1, -1, 1, -1, -1, 1, 1, -1]. \tag{2.5}$$

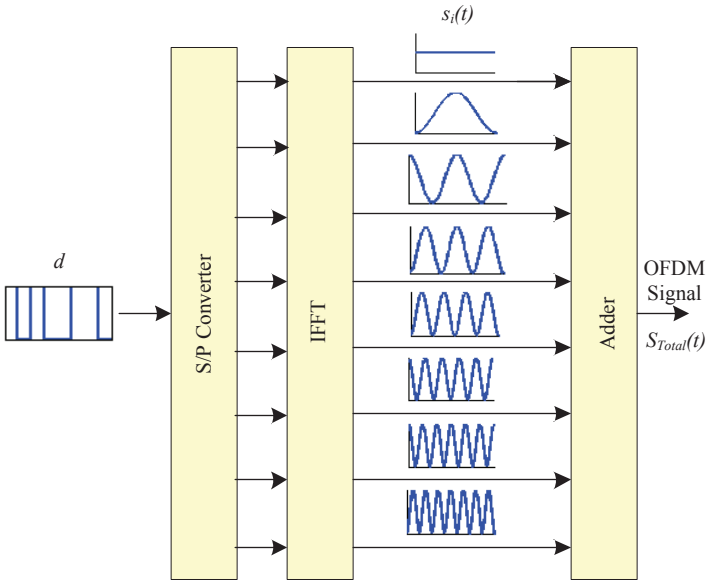

Figure 2.18: Graphical illustration of the procedure of OFDM signal generation with 8 sine waves of different frequencies functioning as subcarriers.

Now, each of the bit d_i will be modulated by a subcarrier of frequency f and its integral multiples, where i = 0,1,2,.....,7. As a result, the individual modulated subcarriers are

$$s_i(t) = d_i * cos(2\pi ft * i). \tag{2.6}$$

As discussed in the seminal paper [62], this can be efficiently performed with the help of Inverse Fast Fourier Transform (IFFT). Figure 2.18 demonstrates the procedure of OFDM signal generation by showing the time domain output waveforms after performing IFFT to achieve subcarrier modulation. All the modulated subcarriers are added together in time domain to form the required OFDM signal, which is mathematically represented as:

$$S_{Total}(t) = \sum_{i=0}^{7} s_i(t). \tag{2.7}$$

Figure 2.19 shows the frequency domain representation of the all the subcarriers independently, as well as that of the composite OFDM signal. All the 8 individually modulated subcarriers can be seen in Figure 2.19 alongwith their resultant OFDM signal.

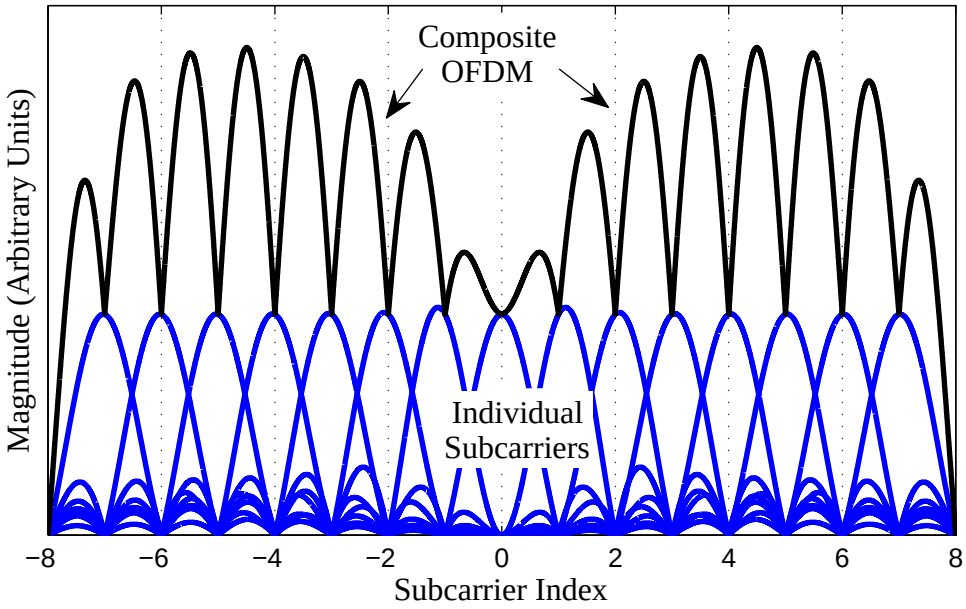

Figure 2.19: Frequency domain representation of all the 8 subcarriers and the composite OFDM signal.

2.3 Non Contiguous Orthogonal Frequency Division Multiplexing (NC-OFDM)

In a majority of the cases of secondary transmission, we will not find a continuous available spectrum to transmit a continuous OFDM signal. In such cases, we have to deactivate subcarriers that are overlapping the spectrum occupied by the primary

user [19]. The information about the subcarriers which are to be switched off is provided on the basis of dynamic spectrum sensing or carrier sensing [66]. This information about the deactivated subcarriers is also provided to the receiver through the transmitted signal. Such OFDM transceiver systems that are capable of turning off the subcarriers and generating non-continuous OFDM signals are called as NC-OFDM transceivers [67]. NC-OFDM is vital from the perspective of Spectrum Pooling because the secondary user has to vacate a frequency as soon as a primary user demands [68]. NC-OFDM is a viable candidate for secondary transmissions of Spectrum Pooling using cognitive radio because of the flexibility that it offers in adjusting its own spectral shape to accomodate the primary user [69].

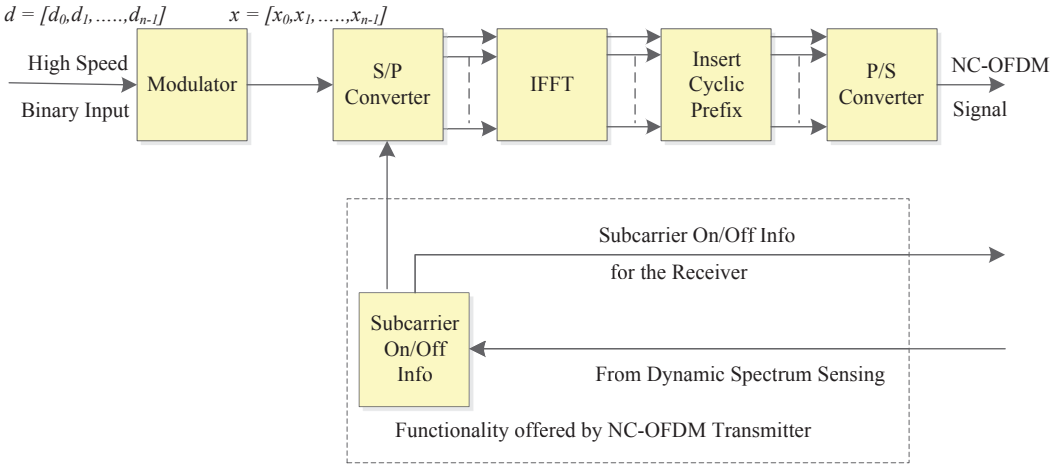

Figure 2.20: General schematic representation of an NC-OFDM Transmitter.

Figure 2.20 shows the general schematic representation of an NC-OFDM transmitter. The NC-OFDM transmitter is similar to the OFDM transmitter shown in Figure 2.14, but with an additional functionality which is specific only to the NC-OFDM. This additional functionality controls the deactivation of the OFDM subcarriers thus

making the OFDM signal non-contiguous. The pattern of subcarrier deactivation is dependent on the spectral occupancy of the primary user which can be found out by dynamic spectrum sensing. This information about the deactivated subcarriers is also given to the receiver via the transmitted signal, in order to enable the receiver to decode the signal correctly.

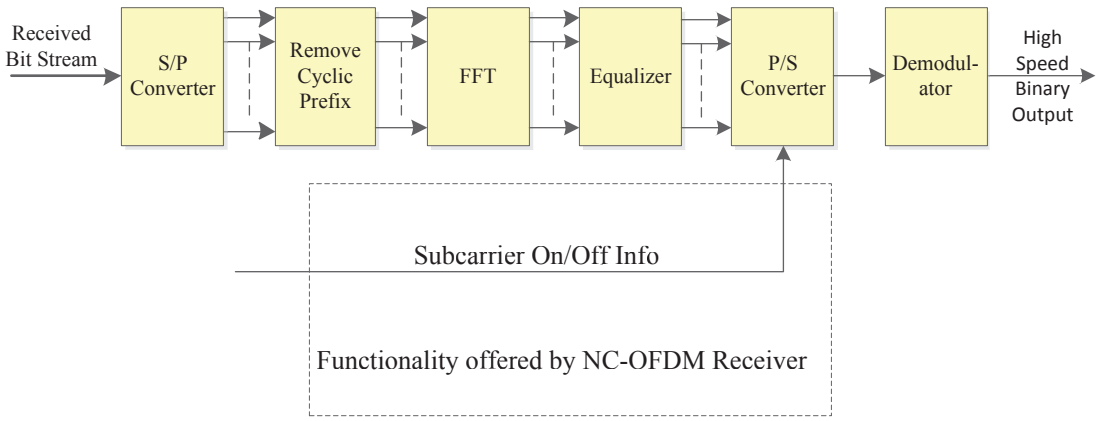

Figure 2.21: General schematic representation of an NC-OFDM Receiver.

Figure 2.21 shows the general schematic representation of an NC-OFDM receiver. The NC-OFDM receiver shown in this Figure is similar to the OFDM receiver shown in Figure 2.17, but with a additional functionality to take care of the deactivated subcarriers. NC-OFDM receiver gets the information about the deactivated subcarriers along with the received signal which is used while decoding the signal.

Let us consider a similar example as shown in Figures 2.18 and 2.19, but with 32 subcarriers instead of 8. In a situation where a primary user demands the frequency range occupied by subcarriers 0-2 and 21-26, the secondary user has to vacate the demanded spectrum. The simplest way would be to stop the entire secondary transmission which would result in vacating the frequencies which could still be used for

transmission. Hence, causing inefficient spectral usage and ultimately, defeating the purpose of spectrum pooling. Instead of doing this, we use the OFDM's flexibility by deactivating the subcarriers that are coinciding with the demanded frequencies. In the considered situation, we deactivate three subcarriers to make room for the primary transmission. Figure 2.22 depicts the spectrum where secondary user deactivates its own subcarriers and creates notches which can be used by the primary user.

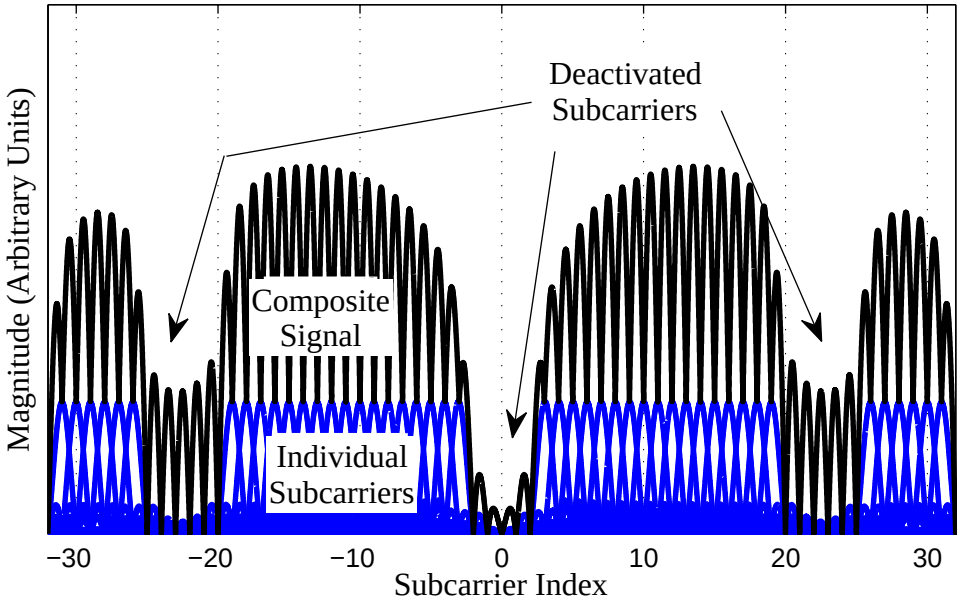

Figure 2.22: An illustration of NC-OFDM for secondary transmissions.

2.4 Out-of-Band Interference Issue in OFDM Transmission

As discussed in the previous sections, OFDM is being considered as an ideal technique for being used with cognitive radio to accomplish Spectrum Pooling. Even

though, OFDM is efficient in filling the spectral gaps left in the licensed spectrum, high out-of-band radiation is a big hindrance in using OFDM for Spectrum Pooling. High out-of-band radiation is a challenge in allowing the coexistence of primary and secondary users in the licensed spectrum wihtout any interference. OFDM uses sinc-type pulses for representing the symbols over the subcarriers. These sinc-type pulses are the source of high sidelobes which ultimately results in interference with the legacy user or even another rental user that are spectrally located adjacent to the unlicensed system. Moreover, in the case of non-orthogonal rental systems, the system performance of the unlicensed system might suffer from this inteference [70]. This section addresses the issue of out-of-band interference in OFDM-based transmissions originating from unlicensed users.

2.4.1 Overview of OOB Interference

The secondary user should cause no interference to the licensed user, is the most crucial condition on which secondary utilization of the licensed spectrum is permitted [12]. Hence, the most important issue that needs to be considered while designing an OFDM-based spectrum pooling is that the impact of secondary usage on the licensed system should be minimal. To achieve this, the primary aim of any algorithm that tries to suppress the sidelobes is to reduce the sidelobe power without affecting the other secondary system parameters [70]. This section briefly describes the mathematical aspect of the interference caused by OFDM-based secondary transmissions.

Consider that *s(t)* is a transmit signal on each subcarrier of the OFDM transceiver system for secondary transmissions. Furthermore, as shown in [71], the *Power Spectral Density* (PSD) of the transmit signal *s(t)* will be mathematically defined as

:

$$\phi_{ss}(f) = A^2 T \left(\frac{\sin(\pi f t)}{\pi f t} \right)^2, \tag{2.8}$$

where A denotes the amplitude of the signal and T representes the total symbol duration which is a summation of symbol duration, T_S, and guard interval, T_G. Now assuming that, the primary transmissions are in the vicinity of the secondary OFDM signal, the mean relative interference, $P_{Interference}(n)$ to a legacy system subband is represented as [18]:

$$P_{Interference}(n) = \frac{1}{P_{Total}} \int_n^{n+1} \phi_{ss}(f)\, df, \tag{2.9}$$

where P_{Total} denotes the total transmit power emitted on one subcarrier and n defines the distence between the considered subcarrier and the legacy system in multiples of Δf.

Figure 2.23 illustrates the interference occuring due to just one OFDM-modulated carrier. It also depicts the subcarrier spacing and the interference power due to the first sidelobe in the first adjacent band. The significant point to be noted from the Figure 2.23 is the high power level of the adjacent sdielobes. It can be observed that, the interference between the subcarrier of the secondary transmission and the considered subband decreases monotonically with the increase in spectral distance between them. This is a characteristic of the *sinc*-type pulse. Moreover, it should be considered that in a practical scenario consisting of N subcarriers, the actual value of interference caused in a particular licensed system subband is a function of the random symbols carried by the *sinc* pulses and N [70].

The concept of calculating the interference caused by one subcarrier of OFDM is being extended to compute the total interference caused by N subcarriers. Let us assume that $s_n(x)$, where n = 1,2,3,.....,N, be the individual OFDM subcarrier of

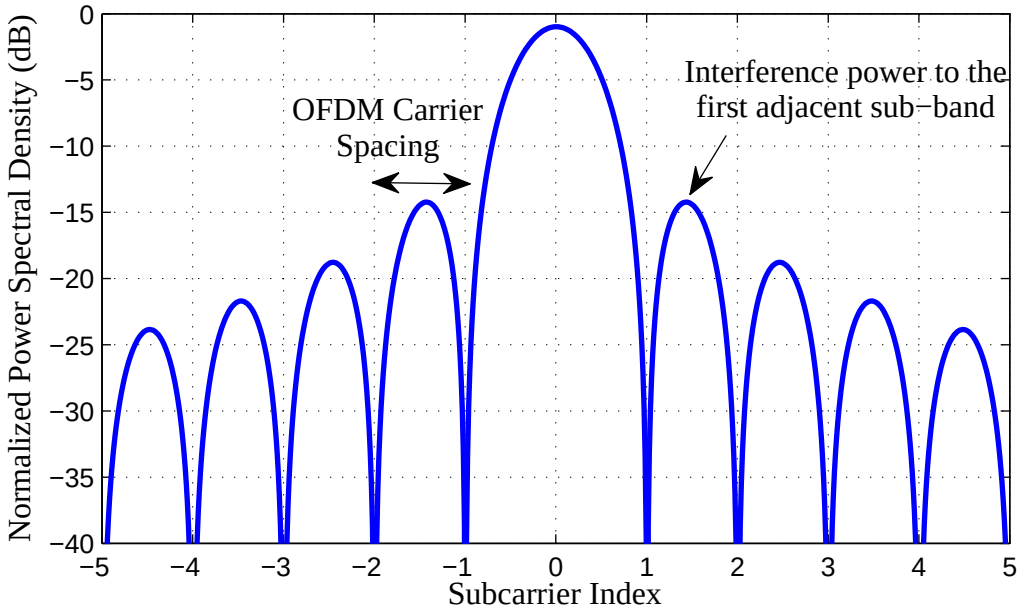

Figure 2.23: An illustration of interference due to one OFDM-modulated carrier.

index n represented in the frequency domain. Then $s_n(x)$ can be represented as:

$$s_n(x) = a_n \frac{\sin(\pi(x - x_n))}{\pi(x - x_n)} \tag{2.10}$$

where, n = 1,2,3,.....,N.

In the Equation (2.10), a_n is a data symbol and x is a normalized frequency given by the formula:

$$x = (f - f_0)T \tag{2.11}$$

where f represents the frequency, f_0 denotes the carrier frequency and x_n defines the normalized center frequency of the n^{th} subcarrier. Consequently, the OFDM signal

in frequency domain and in terms of the subcarriers could be represented as:

$$S(x) = \sum_{n=1}^{N} s_n(x). \tag{2.12}$$

Then, by using the formula of power spectral density and substituting Equation (2.10) and Equation (2.12) into it will result into the power spectral density being represented as:

$$\phi_{ss}(f) = |S(x)|^2 = \left| \sum_{n=1}^{N} a_n \frac{\sin(\pi(x - x_n))}{\pi(x - x_n)} \right|^2. \tag{2.13}$$

Consider a BPSK modulated OFDM based signal with N=8 subcarriers. The input bit stream, of length 8 bits, is a combination of '1' and '-1'. Figure 2.24 shows the normalized power spectral density of this system. The simulation result is based on average power spectral density of the output of the considered system when provided with 100 random combinations of the input bit stream. From this figure, it can be observed that power of the sidelobes in the vicinity of the OFDM *data carriers* (DCs) is signigicantly high. The power of the first sidelobe neighboring to the DC's is as high as -8dBm. Furthermore, the sidelobe power slowly decreases with an increasing distance from the desired OFDM spectrum in frequency domain. The power of the 25^{th} sidelobe is also as high as -18dB. Hence, appending 15 guard subcarriers to the DCs will also result in significantly high sidelobes, causing interference with the adjacent transmissions. Additionally, 15 guard subcarriers is a huge amount of spectrum to be spent on avoiding interference, expecially since we are trying to achieve spectrum efficiency.

This preceding subsections provide an overivew of various existing techniques that are directed towards countering the interference with the adjacent transmissions.

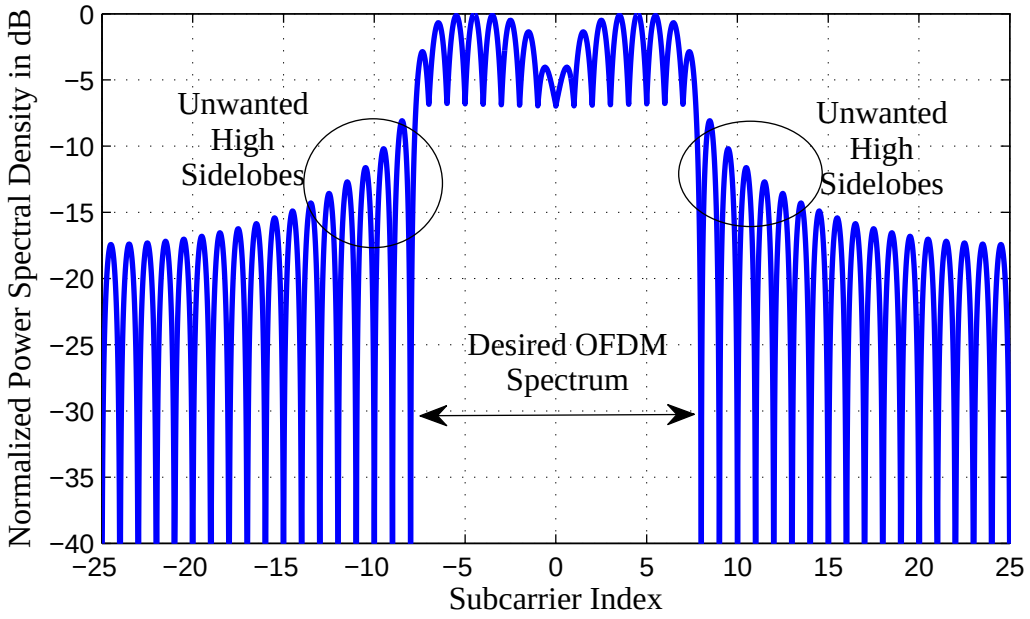

Figure 2.24: An illustration of the interference in BPSK modulated OFDM-based system with N=8 subcarriers.

2.4.2 Guard Bands

Reference [72] proposed a simple technique of using the *Guard Bands* (GBs) to combat out-of-band (OOB) radiation of OFDM-based transmissions. The GBs are nothing but empty or deactivated subcarriers. These GBs are usually placed on the either side of the transmission as shown in the Figure 2.25. By placing the GBs on the edges of the transmission, the signals on either side of the GB do not interact with each other and hence there is no interference. Even though these GBs serves as the buffer between two transmissions, they occupy a significant amount of spectrum. This spectral range used by the GBs could be used for transmission of additional subcarriers, thus increasing the overall throughput. However, their transmission would also result in an increase in the interference. The GBs are not capable of

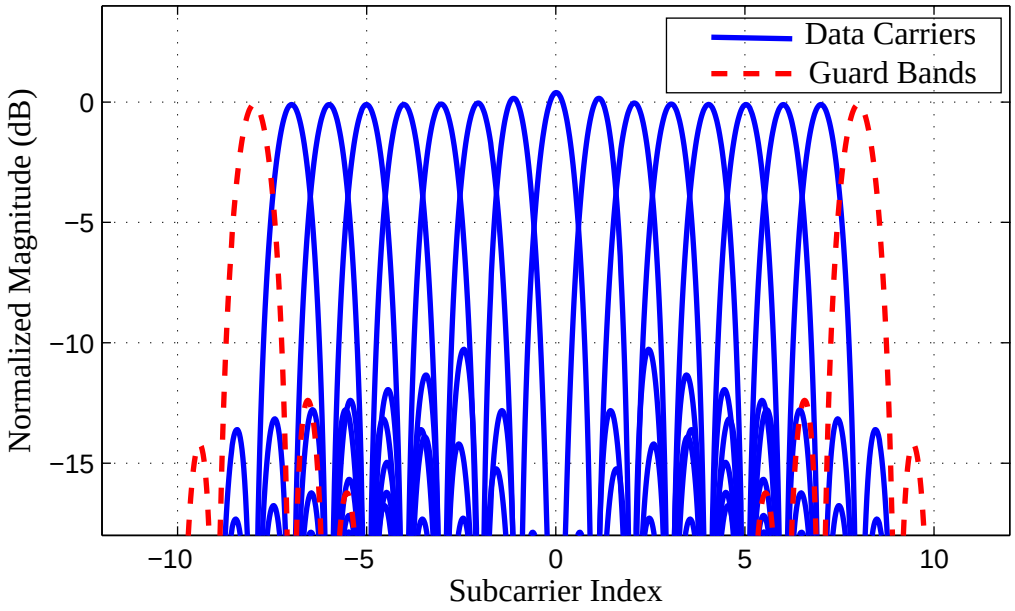

Figure 2.25: An illustration of the use of Guard Band technique for OFDM sidelobe suppression.

suppressing the OOB radiation caused by excessive clipping of the OFDM signal [72]. The suppression achieved with the use of 15 guard bands is around 15dB, as shown in the Figure 2.25, is not sufficient enough to avoid interference and as stated in the previous subsection, this technique does not use the spectrum efficiently.

2.4.3 Windowing

Windowing is a straight forward technique of achieving OFDM sidelobe suppression. As proposed in [73, 18], windowing can be performed on the OFDM transmit signal in the time domain to counter the effects of high sidelobes. As discussed in [34], the sharp transitions between the two adjacent OFDM transmissions is the reason for high OOB radition. Hence, OFDM signal in time domain can be multiplied with

a windowing function to smooth these transitions and ultimately, reducing the OOB radiations. The most commonly used windowing function is raised cosine window, which is defined as [18]:

$$w(t) = \begin{cases} \frac{1}{2} + \frac{1}{2}\cos\left(\pi + \frac{\pi t}{\beta T}\right), & \text{for } 0 \leq t < \beta T \\ 1, & \text{for } \beta T \leq t < T \\ \frac{1}{2} + \frac{1}{2}\cos\left(\frac{\pi(t-T)}{\beta T}\right), & \text{for } T \leq t < (1+\beta)T \end{cases} \tag{2.14}$$

where, β refers to the roll-off factor. Figure 2.26 shows the time domain representation of the raised cosine window function for several values of roll-off factor. For

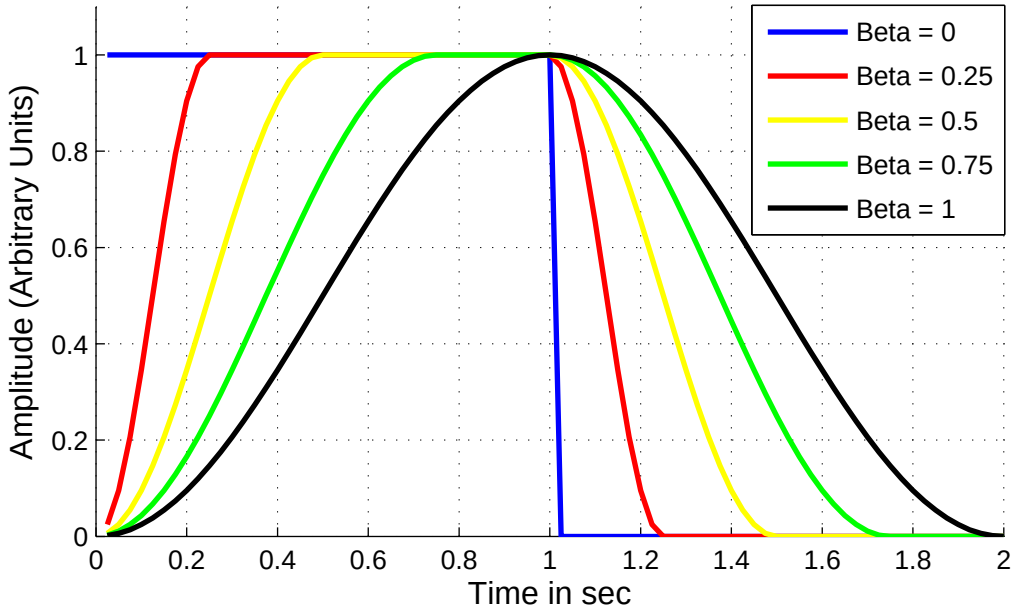

Figure 2.26: Time domain representation of the raised cosine window function for several values of roll-off factor.

the roll-off factor of 0, the raised cosine window functions as a conventional rectangular window. Figure 2.26 shows that as compared to the conventional rectangular

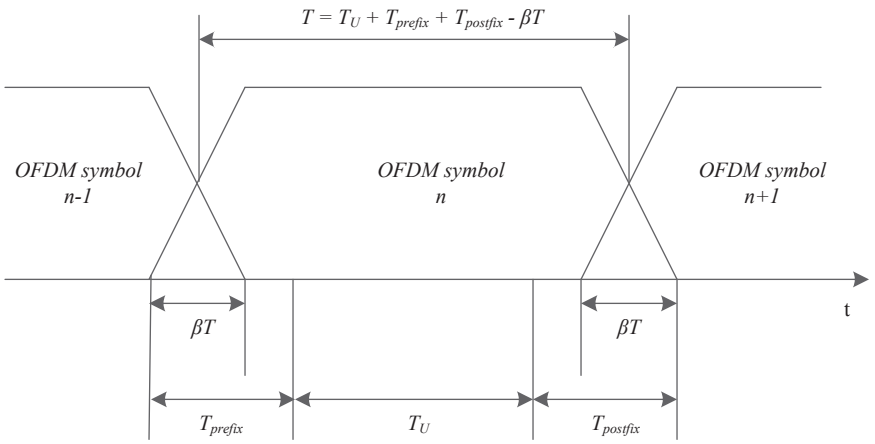

Figure 2.27: Structure of the OFDM signal in time domain using a raised cosine window.

window, edges of raised cosine window are less steep. Therefore, the power in the sidelobes of OFDM subcarriers is much lower than that of the OFDM signal obtained with traditional rectangular windowing [74].

Figure 2.27 shows the time domain OFDM signal after being multiplied by the raised cosine window function. It can be observed from the figure that postfix needs to be longer than βT to maintain the orthogonality of the OFDM signal. In other words, the application of windowing to reduce the OOB radiation of the OFDM signal has the adverse effect of expanding the temporal symbol duration by $(1 + \beta)$, resulting in a lowered system throughput for the unlicensed user.

Also, as depicted in Figure 2.28, higher values of β gives more sidelobe suppression. The symbol duration in time domain increases proportionally with an increase in the roll-off factor, causing reduction in the system throughput. Figure 2.28 illustrates the variation in sidelobe power, caused by the change in roll-off factor. Considering the trade off between the sidelobe suppression and symbol duration,

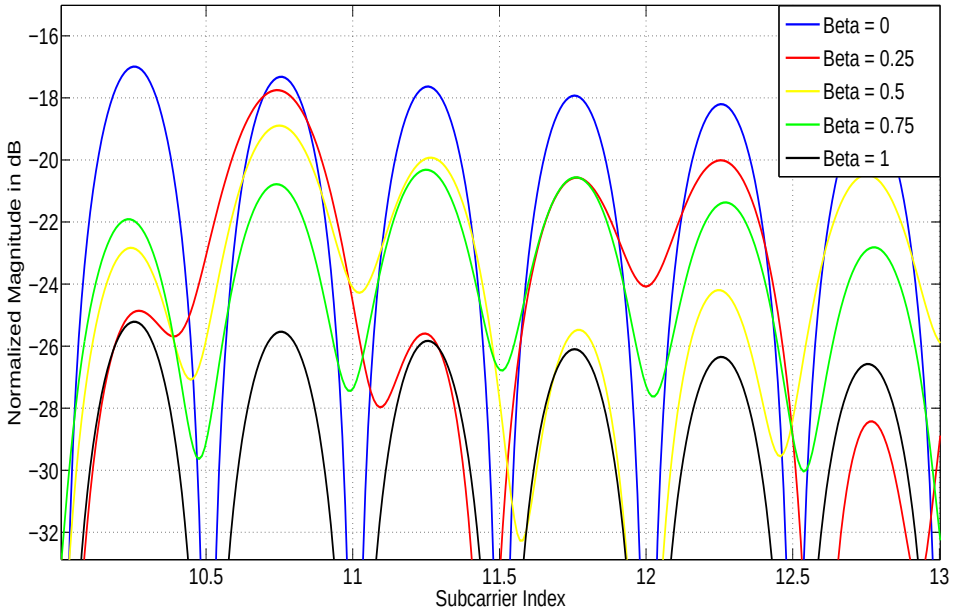

Figure 2.28: An illustration of the variation in sidelobe power of OFDM signal with the change in roll-off factor.

the power of sidelobes is around -20dB for the roll-off factor of 0.75. Nevertheless, windowing can be easily combined with any other sidelobe suppression technique to achieve additional reduction in OOB radiation [34].

2.4.4 Cancellation Carriers

Cancellation Carriers (CCs) is one of the effective technique used to suppress the OFDM sidelobes [75]. In this technique, a carrier wave, which do not possess any data information, is added on the either sides of the OFDM spectrum. As the name

suggests, the amplitude of these CCs is selected such that, they negate the power of the sidelobes, hence lowering the OOB radiation.

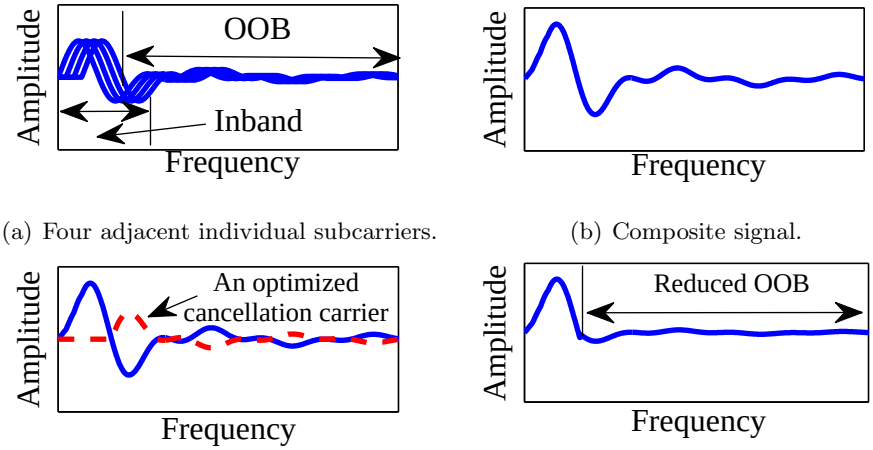

(a) Four adjacent individual subcarriers.

(b) Composite signal.

(c) Composite signal with an optimized CC.

(d) Resultant signal with negligible OOB radiation.

Figure 2.29: Graphical representation of the functioning of cancellation carriers for OFDM sidelobe suppression.

Figure 2.29 illustrates the functioning of the cancellation carriers. Figure 2.29(a) shows four adjacent data carriers and Figure 2.29(b) shows the composite signal formed by these data carriers. Figure 2.29(c) shows an optimized cancellation carrier which tries to negate the power of the sidelobes. The resultant signal obtained after the application of the carrier signal is shown in Figure 2.29(d). As we can see in this figure, the weights on the CCs are optimized in such a way that the resultant of both the signals approaches nullity. There are two algorihms proposed for calculation of the amplitude of CC to cancel out the sidelobe. Optimization-based algorithm was proposed in [75], which calculates the amplitudes of the CCs by solving linear least square problems. Another algorithm to compute the amplitudes of CCs was proposed in [76], which is mathematically less complex than the later one. Simulation

results show that both the algorithms are successful in achieving a 15dB sidelobe attenuation of OFDM signal given 64 subcarriers [2]. Also, as certain amount of transmission power is spent on generation of CCs, there is a small loss in bit error rate performance[76].

2.4.5 Constellation Expansion

This technique of Constellation Expansion, which was proposed in [33], makes use of the fact that different symbol sequences have different sidelobe power associated with it. As proposed in this article, the symbol sequence with least sidelobe power is selected for transmission instead of the generated symbol sequence. In the *Constellation Expansion* (CE) approach, symbols of a modulation scheme that consists of 2^k constellation points are mapped to a expanded modulation scheme that has 2^{k+1} constellation points. Figure 2.30 explains this concept with an example of mapping a BPSK to a QPSK scheme. Let us assume that the two constellation points of BPSK scheme are 'a' and 'b'. As shown in the Figure 2.30, each of these points are mapped to two distinct points of QPSK constellation. To be precise, 'a' is mapped to '*a1*' and '*a2*' while 'b' is mapped to '*b1*' and '*b2*'. At the receiver end, both '*a1*' and '*a2*' are decoded as 'a' without any side information. At the transmitter, a mathematically complex algorithm compares the sidelobe power levels of '*a1*' and '*a2*', and transmits the one with least sidelobe power instead of transmitting 'a'. As a result, achieving the sidelobe suppression. The mapping of points from lower constellation to higher constellation, allows to take the advantage of the randomness in selecting one of the two points as well as the combinations of different in-phase and quadrature-phase components from all the subcarriers would result in selection of the symbol sequence with least sidelobe power. The lone trade-off that is to be considered while using

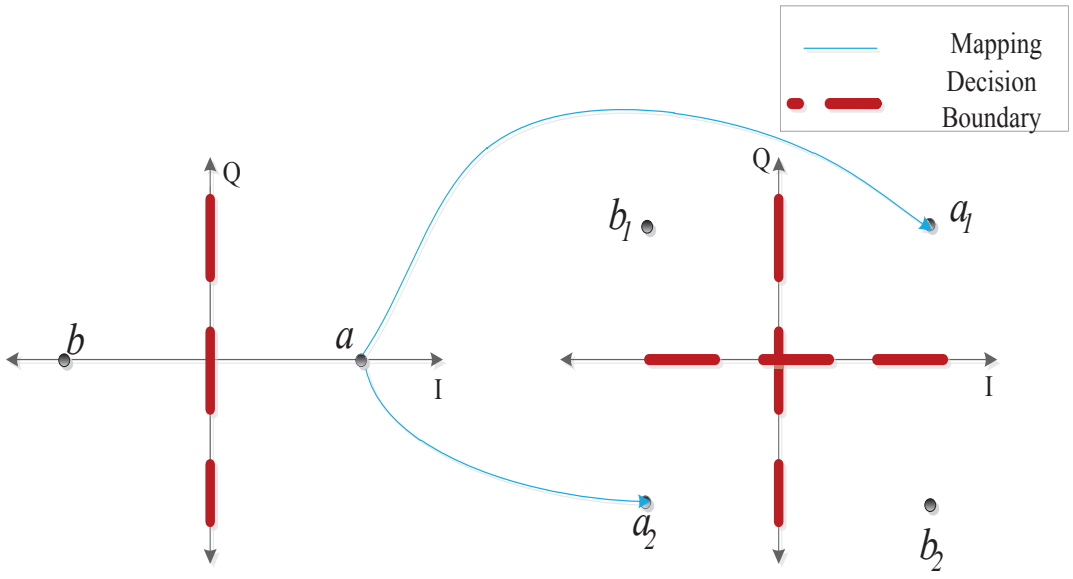

Figure 2.30: Graphical representation of the functioning of constellation expansion mapping for OFDM sidelobe suppression.

CE technique is the increase in bit error rate caused because of the use of higher constellation scheme. This technique provides a sidelobe suppression of 13.2dB for mapping a 2-point constellation to a 4-point constellation [2].

2.4.6 Subcarrier Weighting

Another sidelobe suppression technique that was proposed in [77], is called as Subcarrier Weighting. In this technique, the used subcarriers are multiplied with precomputed subcarrier weights, such that the resultant sidelobes are attenuated. Subcarrier weights used in this technique are the result of a complex optimization technique and they are calculated in such a way that the multiplication of these weights with the used subcarriers result in the subcarriers cancelling eachother in

the sidelobe region. The achieved sidelobe suppression is dependant on the ratio g_{max}/g_{min}, where g is the subcarrier weight. Figure 2.31 shows the sidelobe suppression using subcarrier weighting. As shown in the Figure 2.31, five subcarriers are considered whose amplitudes are adjusted to lower the sidelobe power [2]. This technique provides a sidelobe suppression of 13.45dB when the ratio g_{max}/g_{min} equals $\sqrt{6}$ [77]. Even though this technique does not require transmission of any side information, it suffers a loss in bit error rate because different subcarriers receive different amounts of transmit power.

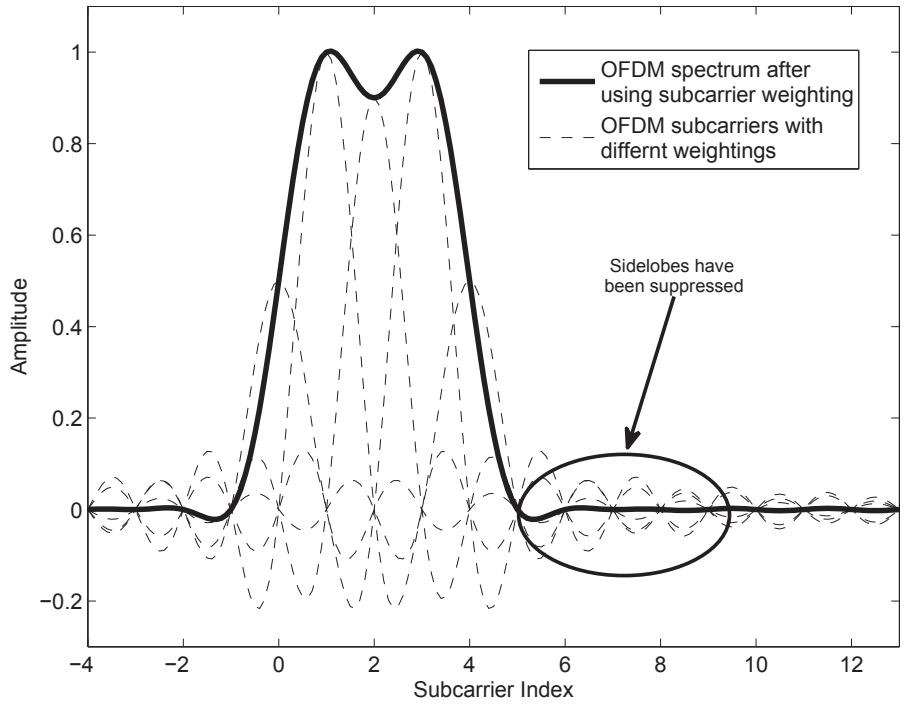

Figure 2.31: Graphical illustration of sidelobe suppression using subcarrier weighting [2].

2.4.7 Performance of the Existing Sidelobe Suppression Techniques

Table 2.3 compares the performance all the existing sidelobe suppression techniques discussed earlier in this chapter [2]. There are total 12 BPSK subcarriers considered in this case and the reduction value of 12^{th} sidelobe compared to the original OFDM sidelobe is shown in the table. As seen in the Table 2.3, all techniques are capable of providing certain attenuation of the sidelobes. However, none of them are able to provide sufficient attenuation so as to allow adjacent transmission of rental and legacy users without any interference. As mentioned in the reference [22], sidelobes should be suppressed to a power level of -60dB with respect to the OFDM spectrum to achieve adjacent transmissions without any interference. The techniques discussed in this chapter are able to provide an attenuation only of around 15dB.

Table 2.3: Chart comparing the performances of existing sidelobe suppression techniques [2].

	Suppression Achieved (dB)	Computation Complexity
Guard Bands	15dB[1]	Low
Windowing	15dB[2]	Low
Cancellation Carrier	24.5dB[3]	Medium
Constellation Expansion	25.2dB[4]	High
Subcarrier Weighting	22dB[5]	Medium

2.5 Chapter Summary

This chapter explains the procedure of generation of basic OFDM signal with a simulink model. It shows how a OFDM system can be modified to generate a

[1] 15 Guard Band subcarriers are required
[2] for roll-off factor of 0.1
[3] with 2 CCs at each side
[4] mapping 2-constellation to 4-constellation
[5] when $g_{max}/g_{min} = 2$

NC-OFDM signal. USRP2 platform for over-the-air transmission of signals generated in simulink is also discussed in this chapter. This chapter gives a mathematical explaination of the interference caused because of the high sidelobes of OFDM spectrum. It also provides an overview of all the existing sidelobe suppression techniques as well as the combination of these techniques which provide better performance. Even though these techniques are successful in providing sidelobe suppression, the attenuation achieved is not sufficient in avoiding interference. Following chapter discusses the techniques to improve OOB sidelobe suppression.

Chapter 3

Proposed OOB Suppression Techniques Via Filtering and Windowing

This chapter provides the detailed explanation of two techniques proposed to attenuate the high sidelobes of OFDM. The first technique uses a series of cascaded Band Reject Filter (BRF) with Finite Impulse Response (FIR) to suppress the high sidelobes. The BRFs are designed using Least Square linear-phase FIR design technique. The proposed technique achieves sufficient sidelobe suppression without using complex mathematical computations and any side information while transmitting. The second technique uses the combination of filtering and raised cosine windowing to suppress the sidelobes.

3.1 Proposed Cascaded Band Reject Filtering Technique

In this section, a novel technique of using a series of cascaded band reject filters to suppress the OFDM sidelobes which cause high Out-of-band(OOB) radiation is discussed in detail. This technique does not use on any complex algorithms or mathematical operations to attenuate the sidelobes. Furthermore, this technique facilitates the OOB suppression without significantly affecting the transmitter/receiver design. The proposed technique is to be applied for an OFDM or NC-OFDM transmitter. Experimental results are also shown in the next chapter to prove the efficiency of the technique to provide the desired suppression.

3.1.1 Schematic of an NC-OFDM Transmitter Employing Cascaded Band Reject Filtering

Figure 3.1 shows a general schematic of OFDM transmitter employing a series of cascaded Band Reject Filters (BRFs) to suppress the high sidelobes. The NC-OFDM transmitter shown in the Figure 3.1 is same as the NC-OFDM transmitter shown in the Figure 2.20 but with an addition of one block, *"Cascaded Band Reject Filters"*. This block accepts the entire NC-OFDM signal and the information about the deactivated subcarriers. Based on the information received about the deactivated subcarriers, the NC-OFDM signal is passed through a series of BRFs, where each BRF acts on a notch in NC-OFDM and further suppresses it. The internal structure of the block *"Cascaded Band Reject Filters"* is shown in the Figure 3.2. It consist of a series of *"N"* BRFs whose coefficients are altered depending upon the input *"Subcarrier On/Off Info"*. Initially, all the filters are set to perform "All pass" function *i.e.*, they will pass the signal as it is. After receiving the information

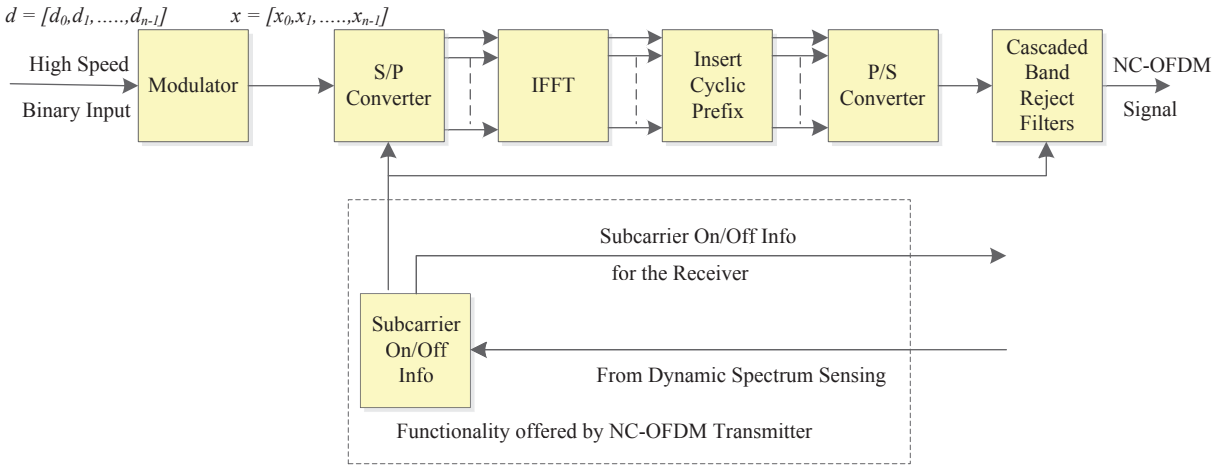

Figure 3.1: General schematic of NC-OFDM Transmitter employing cascaded band beject filters for sidelobe suppression.

about the deactivated subcarriers, the filter coefficients are set such that each BRF suppresses a set of adjacent subcarriers that are deactivated. Thus, each BRF works on a particular notch. The receiver for this NC-OFDM system will be same as the one shown in the Figure 2.21.

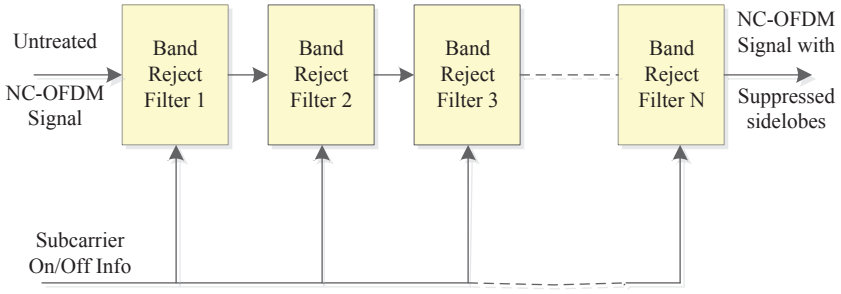

Figure 3.2: General schematic of the cascaded band beject filters used for sidelobe suppression.

The proposed technique first analyzes the information received about the deacti-

vated subcarriers to find the location and the width of all the notches present in the NC-OFDM signal. Secondly, based on this analysis it applies an appropriate series of cascaded BRFs to suppress the notches in the NC-OFDM signal further. Figure 3.3 shows a graphical representation of the effect of the proposed approach on the sidelobes of NC-OFDM. As shown in the Figure 3.3, we should get an additional suppression of the sidelobes after application of the proposed technique.

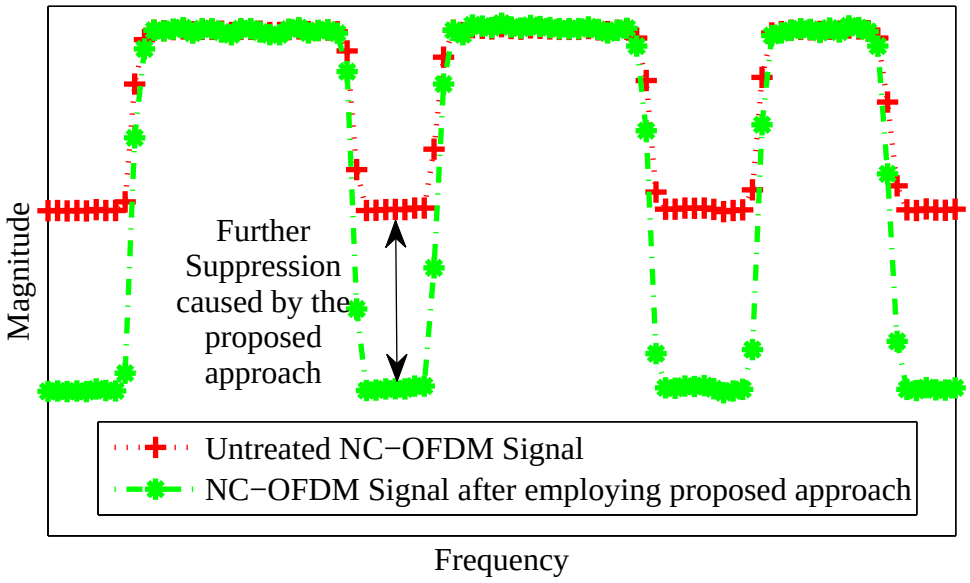

Figure 3.3: Graphical representation of the effect of the proposed approach for sidelobe suppression.

3.1.2 Proposed Sidelobe Suppression Technique

The technique proposed in this thesis functions in two stages. Firstly based on the width and the location of the notch in the NC-OFDM signal, it designs a series of optimized Band Reject Filters (BRFs). Secondly, it applies the cascaded

BRFs to the NC-OFDM signal to achieve further attenuaion of the notches. Figure

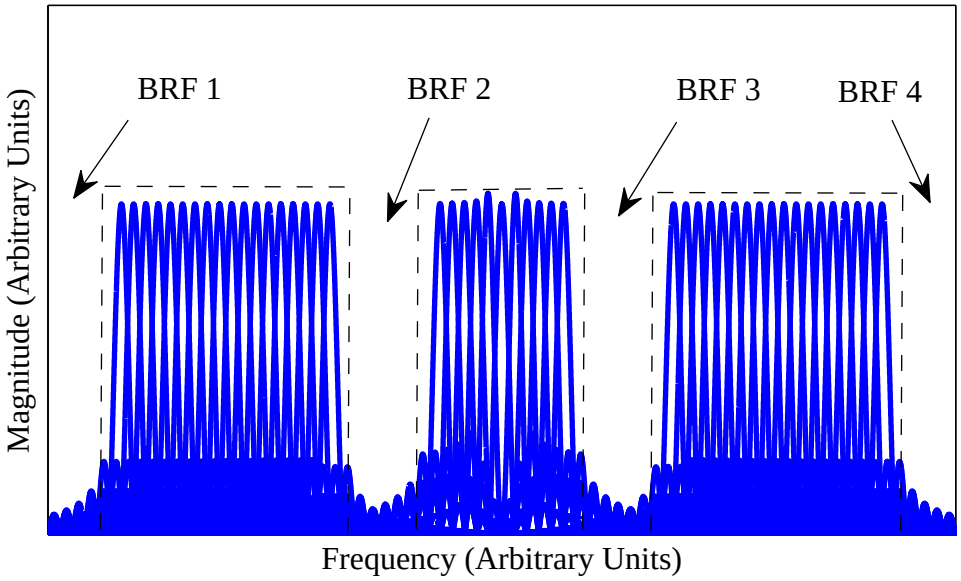

Figure 3.4: An illustration of the functioning of the cascaded band reject filters for sidelobe suppression.

3.4 shows an illustration of the functioning of the cascaded BRFSs for NC-OFDM sidlelobe suppression. As shown in the Figure 3.4, four BRFs are employed to further supress the four notches in the NC-OFDM signal. This technique makes use of a Finite Impulse Response (FIR) filter for suppressing the unwanted sections of the secondary transmissions. Least Square Linear-phase filter design technique is employed to design the FIR filter used for sidelobe suppression. Designed FIR filter minimizes the weighted, integrated squared error between an ideal piecewise linear function and the magnitude response of the filter over a set of desired frequency bands.

A conventional BRF is a two-sided filter that filters out the band of frequencies

on both the sides of the center frequency, f_{center}. Hence, the subcarriers on the either side of the f_{center} will get suppressed by the use of conventional BRF. To solve this problem, we use the technique of *complex exponential modulation*. First, we create a conventional High Pass Filter (HPF) and then we modulate it to act as a one-sided BRF.

3.1.2.1 Designing the HPF

To design a one-sided BRF we create a high pass FIR filter with the desired cut-off frequency. The number of subcarriers deactivated determines the width of the notch which further defines the value of cut-off frequency. Let us consider a NC-OFDM signal comprising of N subcarriers and out of them m subcarriers are deactivated. If these m subcarriers are located such that $m/2$ subcarriers fall on either side of the center frequency, f_{center}, then the cut-off frequency $f_{cut-off}$ is given by the formula:

$$f_{cut-off} = \frac{m\pi}{N}. \tag{3.1}$$

Figure 3.5 shows the magnitude response of the High Pass Filter (HPF) designed with the cut-off frequency given by Equation (3.1). As shown in the Figure 3.5, we have N subcarriers out of which m are deactivated and the HPF is designed such that it supresses the m deactivated subcarriers.

3.1.2.2 Modulating the HPF to create one-sided BRF

To create a one-sided BRF, we will modulate the HPF to the desired location. Let us consider that the filter coefficients of the designed HPF are stored in an array b. Furthermore, let the order of the designed HPF be n. To perform complex exponential modulation on the designed HPF, we create a new set of filter coefficients

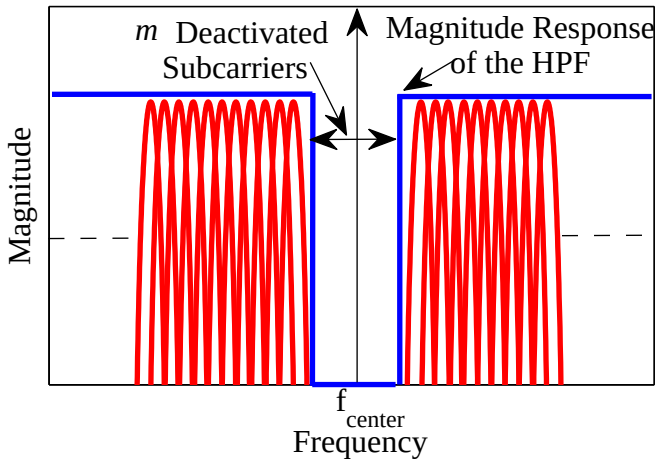

Figure 3.5: Graphical representation of the magnitude response of the HPF designed with the cut-off frequency given by Equation (3.1).

using the formula:

$$b_{mod} = b \exp\left[j\pi x(0:1:n+1)\right], \tag{3.2}$$

where, x takes a value in the range [-1,1] and decides the location of the notch, '-1' being the leftmost location and '+1' being the righmost. b_{mod} and b are same for $x=0$. With an appropriate value of x, we can modulate the conventional HPF to act as one-sided BRF. On convolving b_{mod} with the untreated NC-OFDM signal, we apply the modulated filter to the NC-OFDM signal and attenuate the deactivated subcarriers further. Figure 3.6 shows one such scenario where we have m deactivated subcarriers on the right side of the center frequency. By selecting a suitable value of x, we modulate the HPF to function it as a one-sided BRF and further deactivate those m subcarriers.

In similar manner, we can generate more than one BRFs and cascade them in series to attenuate non-consecutive and varied number of deactivated subcarriers.

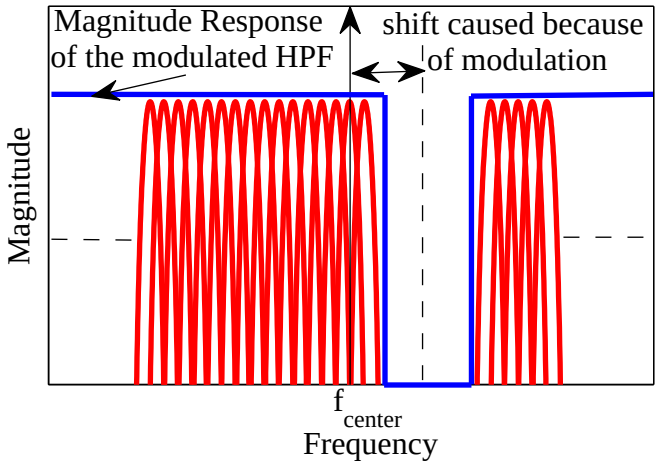

Figure 3.6: An illustration of the modulation of the HPF to make it function as a one-sided BRF.

3.2 Proposed Combined Cascaded Band Reject Filtering and Windowing Technique

This section provides another novel technique for suppression of the high sidelobes of an OFDM signal. The proposed technique uses the combination of windowing and filtering-based approach for sidelobe suppression. Even though windowing alone fails to provide sufficient attenuation, the combination of windowing and filtering-based approach provides better results than both the techniques employed individually. This technique exploits the fact that windowing smoothens the transitions at the end of the OFDM signal, thus reducing the ISI. This technique also results in further attenuation of the deactivated subcarriers, in the case of NC-OFDM. Experimental results shown in next chapter proves the competency of this technique to achieve adequate sidelobe suppression.

3.2.1 Schematic of an NC-OFDM Transmitter Employing Cascaded Band Reject Filtering and Windowing

Figure 3.7 shows the schematic of a NC-OFDM transmitter employing cascaded Band Reject Filters and Raised Cosine Window to suppress the high sidelobes. The NC-OFDM transmitter shown in the Figure 3.7 is same as the NC-OFDM transmitter shown in the Figure 3.1 but with an addition of one block, *"Raised Cosine Window"*.

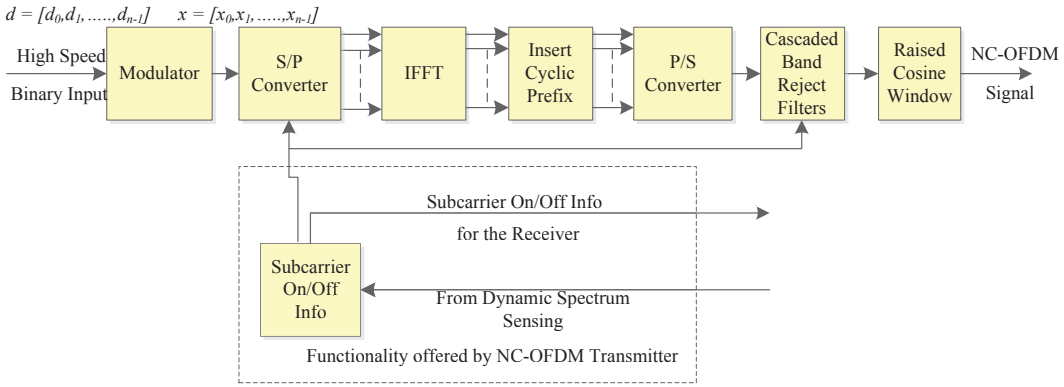

Figure 3.7: General schematic of NC-OFDM Transmitter employing cascaded band reject filters and raised cosine window for sidelobe suppression.

A windowing functions smoothens the sharp transitions between the two adjacent NC-OFDM signals which results in the reduction of sidelobe power level. The raised cosine window is chosen for this purpose over the conventional rectangular window since its edges are less steep than the latter one.The receiver for this NC-OFDM system will be same as the one shown in the Figure 2.21.

Figure 3.8 shows a graphical representation of the effect of the proposed approach of employing the combination of cascaded BRFs and Raised Cosine Window on the sidelobes of NC-OFDM. As shown in the Figure 3.8, we should get an additional suppression of the sidelobes after application of this proposed technique.

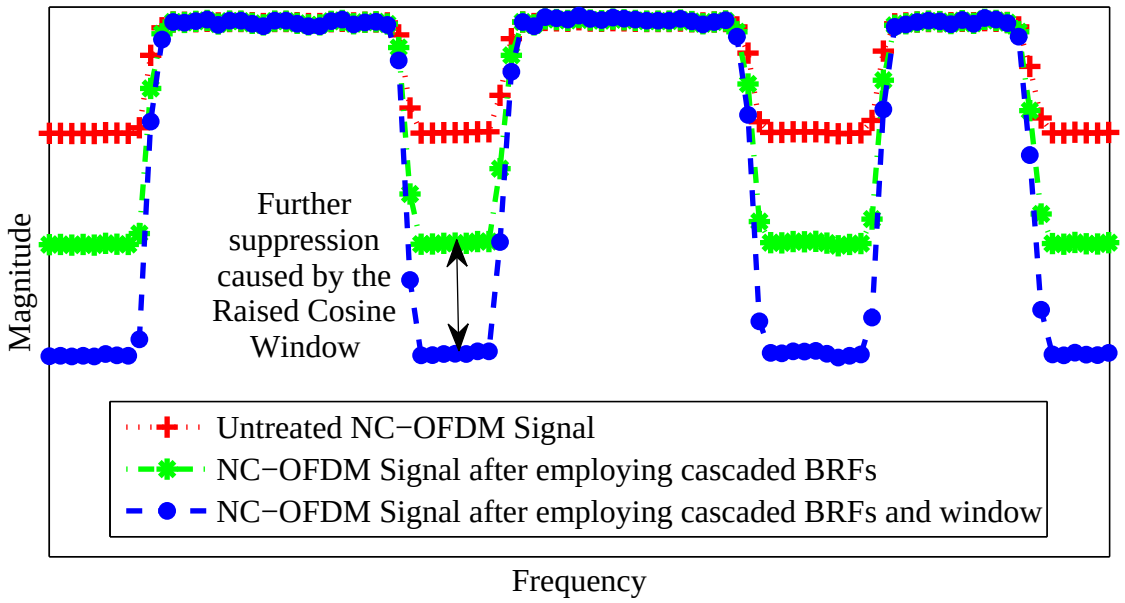

Figure 3.8: Graphical representation of the effect of the combination of BRFs and window on sidelobe suppression.

3.2.2 Proposed Technique of combining cascaded BRFs and Raised Cosine Window

From the Equations (2.10) and (2.13) the *Power Spectral Density* (PSD) of an individual subcarrier in the NC-OFDM signal can be simplified as:

$$\phi_n(f) = K sinc^2((f - f_n)T_s), \tag{3.3}$$

where K is a constant determined by the input bit stream, *'sinc'* is the sinc function defined as sinc(x) = sin(πx)/πx, f_n is the center frequency of the subcarrier, and T_s is the OFDM symbol duration. With these given specifications, the PSD of the NC-OFDM signal can be represented as:

$$\phi(f) = \sum_n \phi_n(f), \tag{3.4}$$

where index n represents all active subcarriers.

'Sinc-pulse' has relatively high sidelobes which causes the out-of-band energy to be significantly high. This *sinc* shape of the subcarrier spectrum is caused because of the sharp transitions among the successive OFDM symbols. These sharp transitions can be avoided by employing a raised cosine window which is given by the equation:

$$w(t) = \begin{cases} \frac{1}{2} + \frac{1}{2}\cos\left(\pi + \frac{\pi t}{\beta T}\right), & \text{for } 0 \leq t < \beta T \\ 1, & \text{for } \beta T \leq t < T \\ \frac{1}{2} + \frac{1}{2}\cos\left(\frac{\pi(t-T)}{\beta T}\right), & \text{for } T \leq t < (1+\beta)T \end{cases} \tag{3.5}$$

where, β refers to the roll-off factor. Figure 3.9 shows the power spectral density of one subcarrier of an OFDM signal for different values of the roll-off factor, β. As shown in the Figure 3.9, the sidelobe power is lower for a higher value of β. However, OFDM signal duration increases in time domain with an increase in the value of β, which causes redution in the system throughput. Hence, while designing the raised cosine window for an OFDM system, a trade-off should be considered between the sidelobe suppression and symbol duration. Even though the sidelobe power seen in Figure 3.9 is significantly high, it is reduced sufficiently by the use of BRFs. Windowing, individually may not be the best choice to reduce sidelobe power, but when combined with the proposed approach of employing cascaded BRFs it gives much better sidelobe suppression.

The use of FIR filters for suppressing the sidelobes also has a adverse effect on the system. As FIR filter uses a very large filter order to provide the required attenuation, applying such FIR filter to the input signal results in stretching of the signal in time domain. This stretching causes narrowing of the signal in frequency domain.

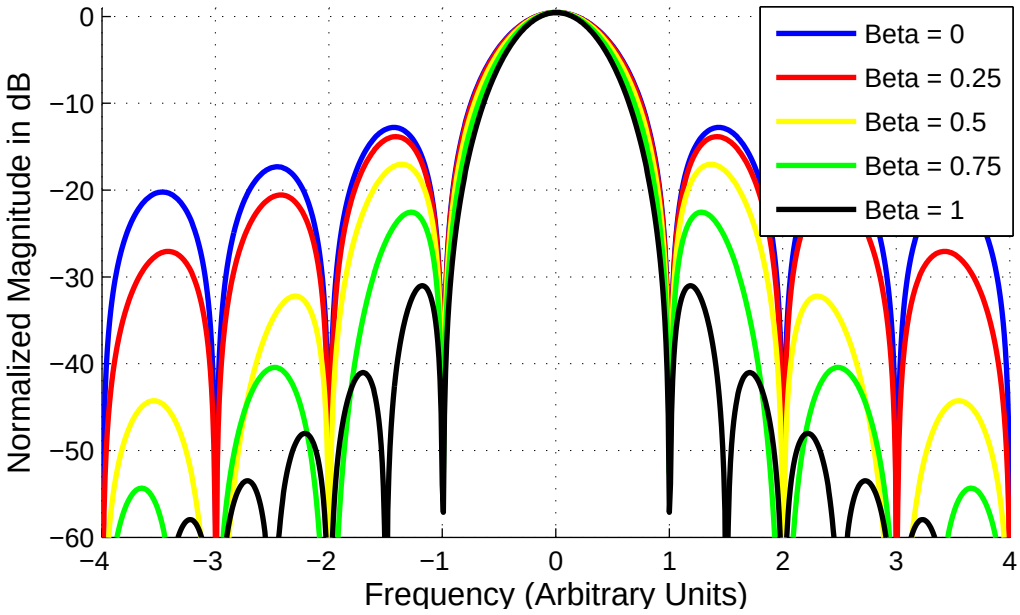

Figure 3.9: The power spectral density of one subcarrier of an OFDM signal for different values of the roll-off factor, β.

3.3 Chapter Summary

This chapter explained both the techniques proposed to redeuce the sidelobes of NC-OFDM signal sufficiently to accomodate both the primary and secondary transmissions without any interference. The first technique uses a Finite Impulse Response (FIR) filter to suppress the high sidelobes. The FIR filter is designed using Least Square linear-phase FIR design technique. The second technique uses the combination of band pass filtering and raised cosine windowing to suppress the sidelobes.

Chapter 4

Over-the-air Experimental Results

This chapter shows the over-the-air experimental results obtained with the proposed techniques of the NC-OFDM sidelobe suppression. It first describes the experimental setup used to obtain all the results. Secondly, the performance of the proposed techniques are compared for variety of NC-OFDM configurations. It also compares the performance of the proposed techniques with the technique proposed in [2].

4.1 Experimental Setup

The experimental results shown in this chapter are obtained using the setup shown in the Figure 4.1. Figure 4.1 shows a schematic representation of the experimental setup for observing the performance of the proposed techniques over-the-air using USRP2 radios. As shown in the Figure 4.1, we have a USRP2 acting as a transmitter. This USRP2 is connected to a computer that generates the desired NC-OFDM signal on the Simulink at the baseband frequency. The USRP2 then transmits the NC-OFDM signal over-the-air using the antennas connected to it. This signal is collected

in the form of electromagnetic radiations by the horn antenna which forward the received signal to the spectrum analyzer.

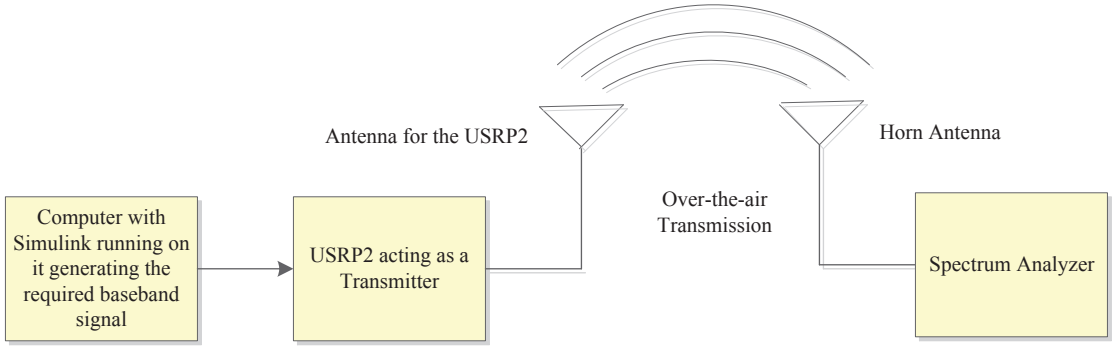

Figure 4.1: Schematic representation of the experimental setup for verifying the performance of the proposed techniques over-the-air.

The NC-OFDM symbols are generated on the Simulink using a Differential Binary Phase Shift Keying (DBPSK) modulation scheme. The number of subcarriers modulated orthogonally is 52, in the case of contiguous signal. The subcarrier bandwidth is kept constant over the entire experiment. All the experimental results are averaged 500 times to attain higher accuracy in the results. The Band Reject Filters (BRFs) employed for sidelobe suppression are designed with an order of 251 and the optimum roll-off factor used for the generation of the raised cosine window is 0.2.

Table 4.1 shows all the detailed specifications used for the entire experiment. These parameters are kept constant over the span of all experiments.

Table 4.1: Specifications used for the generation of NC-OFDM Signal.

Parameter	Specification
Experimental trials for each output	500
Carrier frequency	2.47 GHz
Number of subcarriers	52
Null subcarriers added on either side	10
Length of cyclic prefix	14
Filter order	251
Roll-off factor wor window	0.2
Total Bandwidth	66.5 KHz
Bandwidth of each subcarrier	2.94 KHz

Two spectrum sharing scenarios are considered for creating these experiments. First, when the spectral space occupied by the primary user is contiguous, allowing the secondary NC-OFDM transmission with only one notch. Second, when the bandwidth occupied by the primary user is non-contiguous, resulting in secondary NC-OFDM transmission with variable number of notches, each having a different bandwidth.

This NC-OFDM signal that is generated by the Simulink at baseband frequency is translated to the radio frequency and transmited over-the-air by the USRP2. Figure 4.2 shows the actual experimental setup with all the hardware components used. As shown in the Figure 4.2, the horn antenna captures the electromagnetic radiations over-the-air and gives the signal to the Spectrum Analyzer through the cable connection between them. The Spectrum Analyzer displays the signal received over-the-air.

Spectrum Analyzer is a very sophisticated device that collects data from an antenna and displays it on the screen. Figure 4.3 shows the screen capture of the Spectrum Analyzer featuring its parameters and the received NC-OFDM signal. The two most vital user controlled parameters of the Spectrum Analyzer are the *center frequency* and the *span*. *Span* defines the bandwidth that is to be considered and is

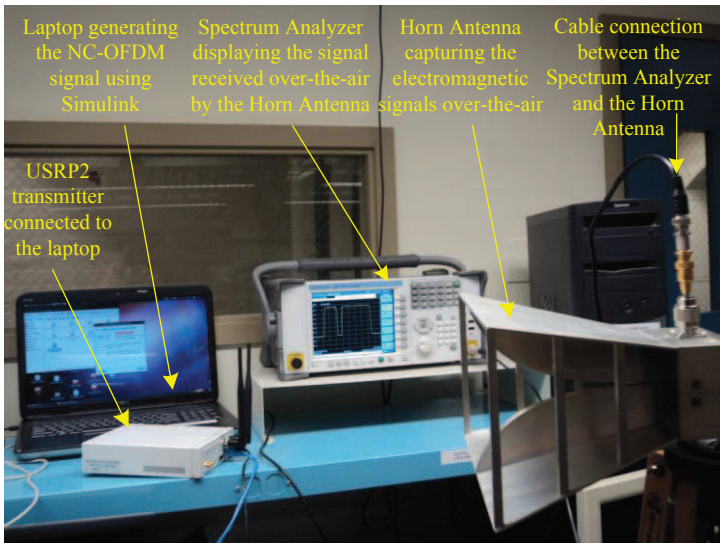

Figure 4.2: Experimental setup for verifying the performance of the proposed techniques over-the-air.

selected such that the entire NC-OFDM transmission falls within its range. $ResBW$ is the resolution bandwidth determines how close frequency components in the signal spectrum can be and still be displayed as distinct components on the screen. VBW stands for Video Bandwidth which essentially reduces the noise displayed, making the power levels easier to see. The pre-amplifier is usually used for weak signals.

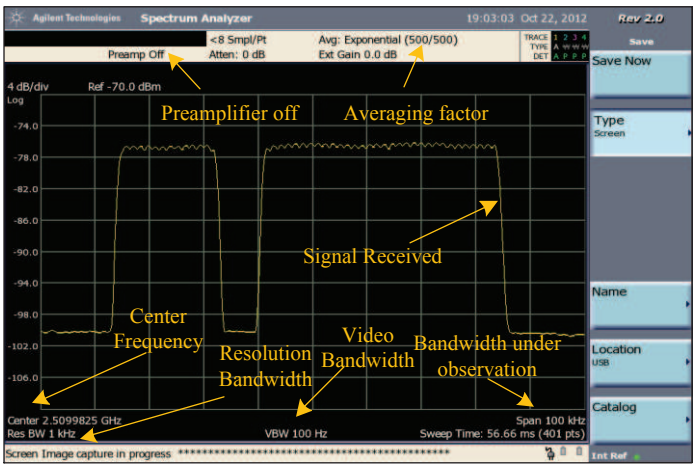

Figure 4.3: Screen capture of the spectrum analyzer showing its user controlled parameters and the received NC-OFDM signal.

4.2 Performance with Notches of Different Sizes

This section compares the performance of the proposed techniques with a change in the size of the notch. It also compares the experimental results with the results obtained by the technique proposed in [2].

Figure 4.4 shows the experimental generation of DBPSK modulated NC-OFDM signal with a medium sized notch, created by deactivation of six subcarriers. This figure compares the untreated NC-OFDM signal with the NC-OFDM signal obtained after application of both the proposed techniques as well as the technique of employing four Cancellation Carriers (CCs) and modulated filterbanks ($\beta = 0.25$) discussed in the reference [2]. It can be seen from the Figure 4.4 that the proposed technique gives a slight better performance than the technique discussed in [2] without any complex mathematical operations or algorithms.

Figure 4.5 shows the 95% confidence bounds for the NC-OFDM signal with fil-

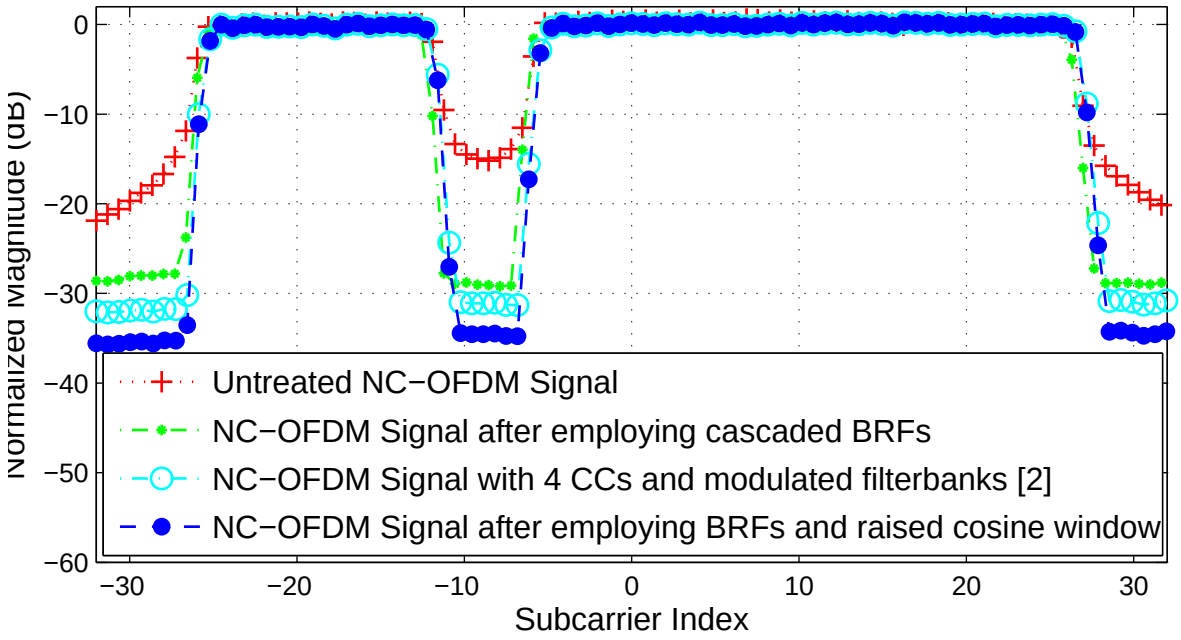

Figure 4.4: An example of an NC-OFDM signal after application of both the proposed techniques as well as the technique discussed in [2] to suppress 6 subcarriers.

tering and windowing to suppress 6 deactivated subcarriers. It can be observed from the Figure 4.5 that the sidelobe power level is in the range [-30dB,-40dB] with a 95% confidence.

Figure 4.6 shows the variation in the performance of both the proposed techniques with the change in width of the notch in the NC-OFDM signal. The amount of sidelobe suppression achieved in decibal (dB) serves as a metric for comparing the performance. It can be observed from the Figure 4.6 that the attenuation of the sidelobes or the performance of the proposed techniques improves with the increase in the width of the notch. Hence, more the number of consecutive subcarriers

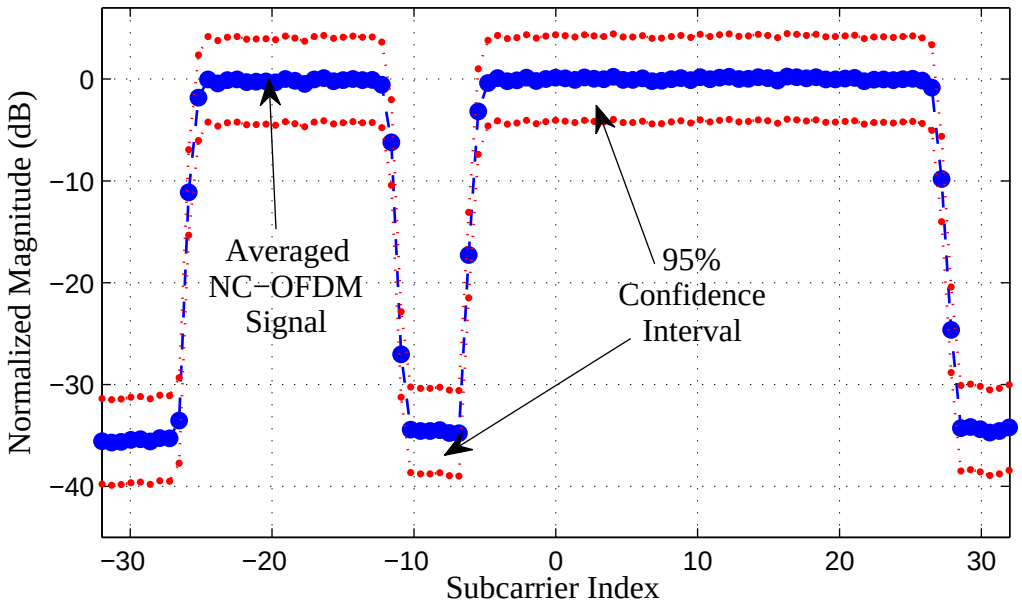

Figure 4.5: Sidelobe suppressed NC-OFDM signal with 95% confidence bound.

deactivated, higher will be the attenuation of the deactivated subcarriers achieved.

Figure 4.7 compares the confidence levels for several different configurations of the NC-OFDM signal. This figure shows the standard deviation of the sidelobe power levels for three configurations of the NC-OFDM signal with different number of subcarriers deactivated. It can be observed from the figure that for NC-OFDM signal with 8 subcarriers deactivated the sidelobe power is less than -35dB with 92% confidence. Similarly, a NC-OFDM signal with 6 subcarriers deactivated has sidelobe power less than -30dB with 92% confidence. All the configurations of NC-OFDM signal has the sidelobe power less than -25dB with 99% confidence.

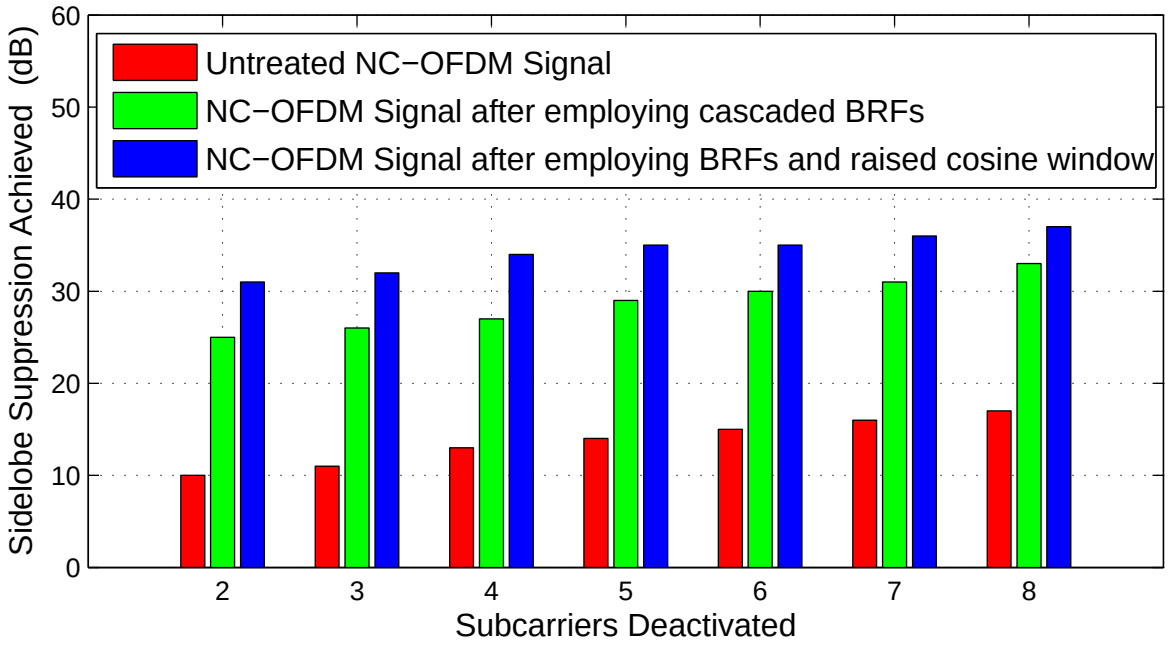

Figure 4.6: Comparison of sidelobe powers with the change in number of subcarriers deactivated in the NC-OFDM signal.

4.3 Performance with Different Number of Notches

Number of notches present in the NC-OFDM signal is also a significant factor affecting the performance of the proposed techniques. This section compares the peformance of both the proposed techniques and the technique discussed in the reference [2] on the basis of different number of notches present in the NC-OFDM signal.

Figure 4.8 shows the DBPSK modulated NC-OFDM signal that has four notches of unequal bandwidths, experimentally generated in four different ways in order to compare the performance of both the proposed techniques with the technique of using 4 CCs and modulated filterbanks with β=0.2 proposed in the reference [2]. Figure 4.8 shows that the sidelobe suppression achieved with more number of unequal notches

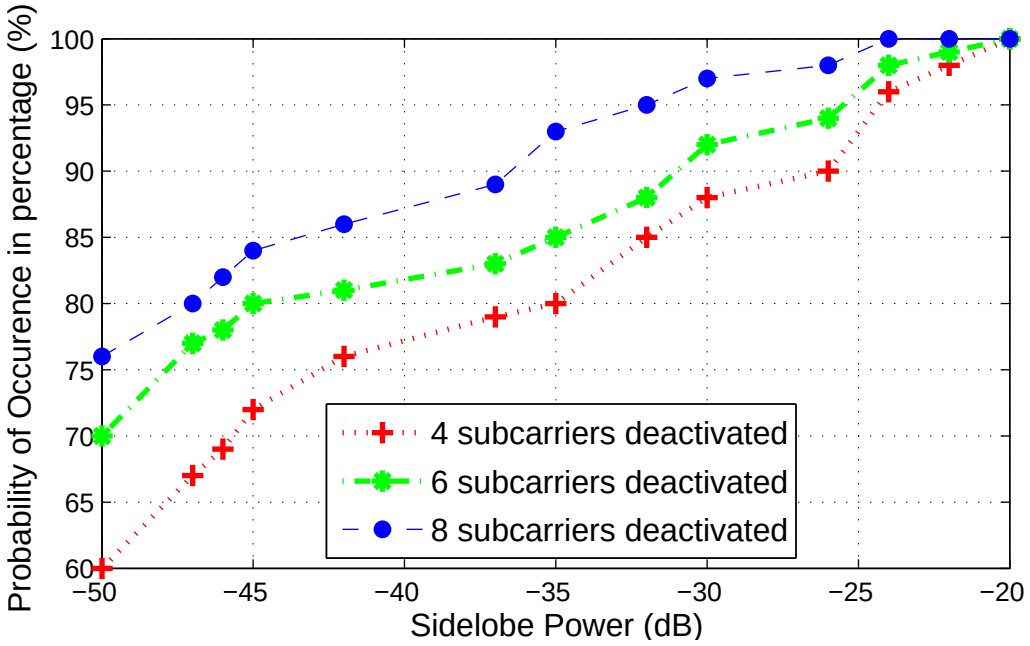

Figure 4.7: Comparison of confidence that the sidelobe power level is below threshold.

is less than that achieved with just one notch showed in the Figure 4.8. Also, the proposed technique performs almost same as the technique proposed in the reference [2] but with much lesser complexity and computation.

Figure 4.9 shows the variation in the performance of both the proposed techniques with the change in number of notches present in the NC-OFDM signal. It can be seen from the Figure 4.9 that the performance of the proposed techniques decreases with an increase in the number of notches.

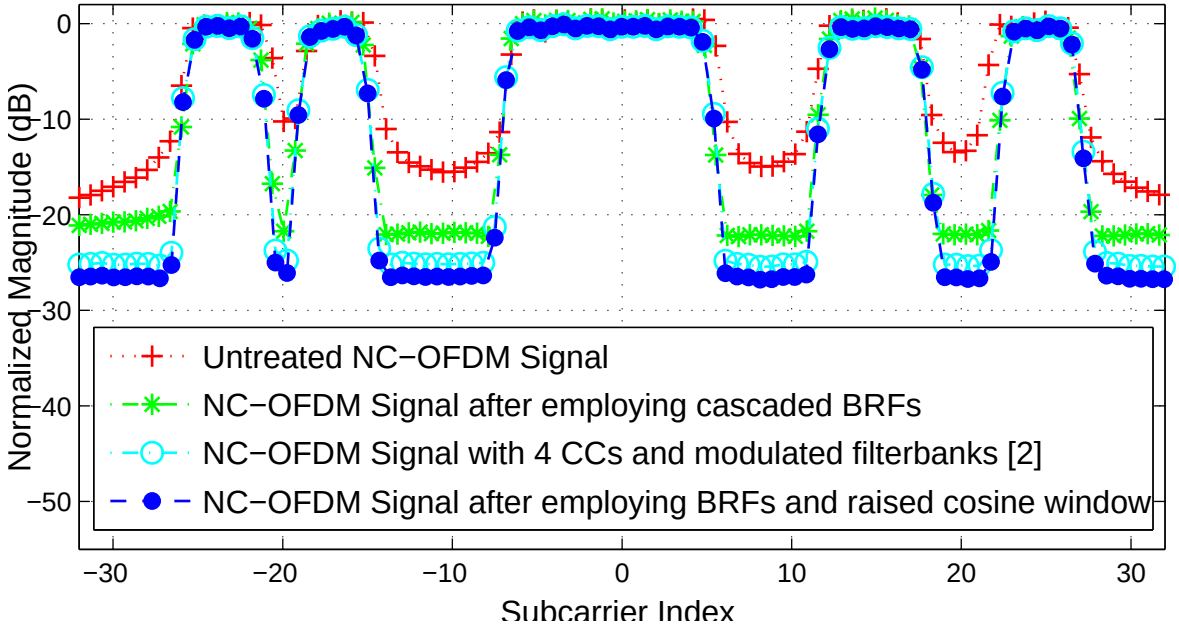

Figure 4.8: An Example of NC-OFDM signal with four notches after application of both the proposed techniques as well as the technique proposed in [2].

4.4 Chapter Summary

This chapter discussed the experimental setup arranged for gathering the results in detail. The experimental setup discussed in this chapter includes configuring the Spectrum Analyzer, specifications of the NC-OFDM signal and the parameters of the proposed techniques. It also shows the experimental results proving the effectiveness of the proposed techniques as well as compares the performance of the techniques for different configurations of the NC-OFDM signal. This chapter also compares the performance of both the proposed techniques with the technique of proposed in the reference [2] for all those NC-OFDM configurations.

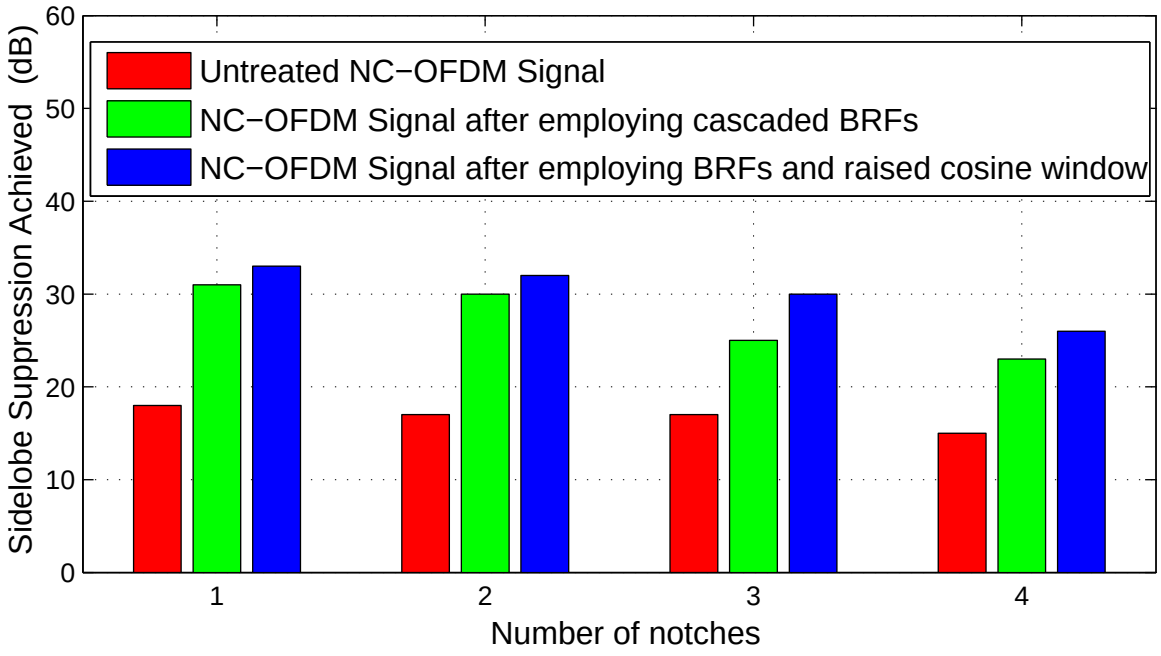

Figure 4.9: Comparison of sidelobe powers with the change in number of notches present in the NC-OFDM signal

Chapter 5

Conclusions

In this thesis, we made an effort to use filtering and windowing for suppression of the high OFDM sidelobes. The attenuation of the high OFDM sidelobes of secondary transmissions is very important for the coexistence primary and secondary users without any interference. The techniques that have been proposed in this thesis are:

- The first proposed technique is the filtering technique which uses a series of cascaded band reject filters (BRFs) to further supress the notches in the NC-OFDM signal. This proposed technique designes a BRF by exponential modulation of a high pass filter (HPF) of desired cut-off frequency. The design of a BRF for this technique is a two stage procedure, wherein a Finite Impulse REsponse (FIR) filter with desired bandwidth is created first and then it is exponentially modulted to the location which coincides with the notch in NC-OFDM signal.

- The second proposed technique uses the combination of windowing and filtering-based approach for sidelobe suppression. Even though windowing alone fails to provide sufficient attenuation, the combination of windowing and filtering-based

approach provides better results than both the techniques employed individually. This technique exploits the fact that windowing smoothens the transitions at the end of the OFDM signal, thus reducing the ISI.

5.1 Future Work

There exists a number of areas for future work related to what is being presented in this thesis.

- Both the proposed algorithms are relying on carrier sensing to find the location of primary user and accordingly generate suitable secondary transmissions. A predictive algorithm can be created which will analyse the spectral usage pattern of primary user over a certain period of time and then predict the location of primary user at any particular time. This will save a significant amount of time which is spent on carrier sensing.

- The existing algorithms as well as those presented in this thesis do not utilize the statistical relationship between the random symbols carried by the subcarriers and the resulting sidelobe power levels. An understanding of such a relationship would greatly help in designing techniques successful in achieving better sidelobe suppression.

- It would be interesting to know the performance of technique which would combine the existing techniques of cancellation carriers, cascaded BRFs and windowing.

- The FIR filters causes stretching of the channel impulse response. The use of Infinite Impulse Response (IIR) filters instead of FIR filters might help in

shortening of the channel impulse response

- A sidelobe suppression technique that employes variable data rates to the subcarriers that are closer to the edges of the OFDM spectrum can be developed. This algorithm is based on an idea, if the subcarrier that are closer to the edge of the OFDM spectrum have slower data rates, then the subcarrier bandwidth would be smaller and the sidelobes emerging from them would also be smaller, leading to low sidelobe power levels.

Appendix A

Simulink Model for NC-OFDM Signal Generation.

The Simulink model shown in the Figure A.1 is used to generate a NC-OFDM signal with 4 notches of variable sizes. The uniform random bit generator serves as the source of high speed input bit stream. A buffer is used to slow down the speed and convert the serial bit stream to a parallel bit stream. A subcarrier controller then accepts these parallel bits and nulls the bits corresponding to the subcarriers that are to be deactivated. Inverse fast fourier transform (IFFT) is then applied to these bits to perform orthogonal modulation followed by addition of the cyclic prefix to form a NC-OFDM signal. This untreated NC-OFDM signal is then passed through a series of cascaded band reject filters (BRFs) to further attenuate the deactivated subcarriers. Finally, the sidelobe suppressed NC-OFDM signal is then given to the transmitter block of Simulink for over-the-air transmission using USRP2 radio platform.

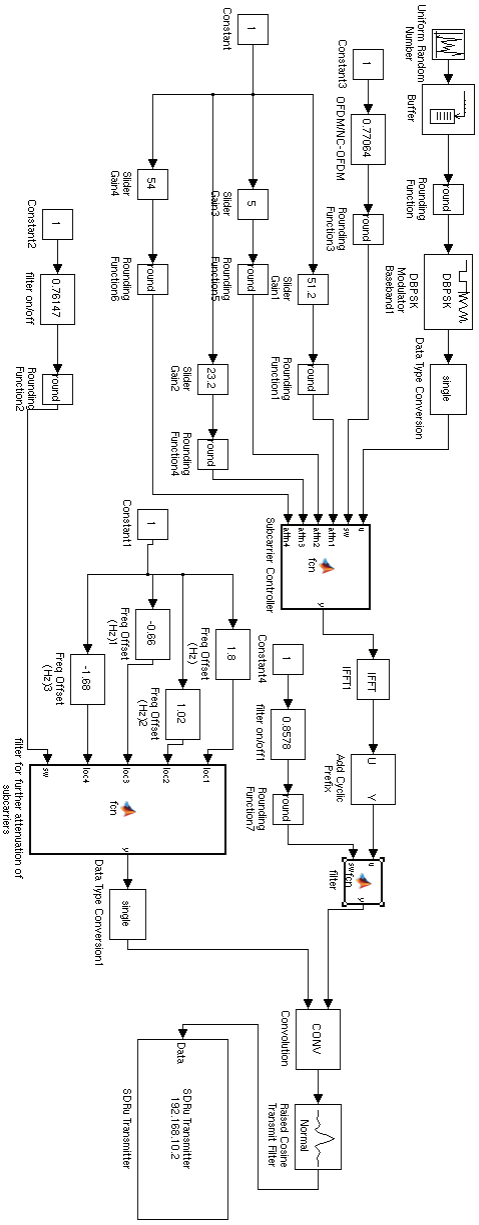

Figure A.1: Simulink model to generate NC-OFDM signal with four notches employing the proposed techniques.

Appendix B

MATLAB function to generate BPF coefficients

This Appendix B shows the MATLAB script used for the generation of BPF coefficients. The input parameters to ths function includes a switch which turns the filters On/Off. If the user decides to turn Off the filters the coefficients of all the BPFs will be a delta function, which implies that the filter will pass the input as it is without any filtering. For the another case, where we want filtering to suppress the sidelobes, there are 4 HPF with varioble cut-off frequencies, selected so as to overlap with the notch exactly. These coefficients of HPF are then exponentially modulated to create the BPF. The modulation factor determines the location of the BPF, which can be adjusted on the fly using te slider gain used in the Simulink model shown in the Figure A.1. These filter coefficients are then convolved with each other to cascade then in a series. The snippet of this MATLAB function is as follows:

function y = fcn(loc1, loc2, loc3, loc4, sw)

% loc1,loc2,loc3,loc4: value between [-π, π]; selects the value for modulation

```
switch sw
% sw acts as a switch to turn the cascaded BRFs On/Off
case 1
% case when filters are turned On
a = firls(251,[0 0.03 0.04 1],[0 0 1 1]);
% 4 high pass filters (HPFs) of variable cut-off frquencies.The cut-off frequencies depends on the width of notces.
c = firls(251,[0 0.11 0.12 1],[0 0 1 1]);
d = firls(251,[0 0.09 0.1 1],[0 0 1 1]);
e = firls(251,[0 0.06 0.07 1],[0 0 1 1]);
otherwise
a = zeros(1,253);
% If BRFs needs to be turned off, select the filter coefficients to be a delta function. This will create a filter that will pass everything
a(1) = 1;
c = a;
d = c;
e = d;
end
b1 = a.*exp(1j.*(loc1).*(0:1:252));
% Perform exponential modulation on the HPF to create BRF. loc is the factor for modulation which defines the location of the filter
b2 = c.*exp(1j.*(loc2).*(0:1:252));
b3 = d.*exp(1j.*(loc3).*(0:1:252));
b5 = e.*exp(1j.*(loc4).*(0:1:252));
```

```
b4 = conv(b1,b2);
% Coefficients of all the BRFs are convolved with each other to cascade them in
a series
b6 = conv(b3,b5);
b = conv(b4,b6);
y = b';
end
```

Appendix C

MATLAB function to deactivate subcarriers

This Appendix C shows the snippet of MATLAB function that accepts the indices of the subcarriers that are to be dectivated and sets the value on this subcarrier to 0. This function is hardcoded to deactivate 2,4,6 or 8 subcarriers neighboring to the subcarrier index provided in the input. Initially, the input bits received are arranged in the format of OFDM. This function also has a switch to turn off the deactivation and generate a contiguous OFDM. If the switch is turned on then it will replace the corresponding bits with 0. The MATLAB function is as follows:

```
function y = fcn(u,sw,attn1,attn2, attn3, attn4)
y = [u(1:26); zeros(10,1); zeros(10,1); u(27:52)];
% Contiguos OFDM signal with 10 zeros appended on either side
if sw  = 0
% switch to shift between OFDM and NC-OFDM
fc1 = round(attn1*15/40);
```

```
fc1 = 72 - fc1;
% Maps the slider gain value to the subcarrier index. '15/40' is the mapping factor.
y(fc1-1:fc1) = zeros(2,1);
% Nulls two subcarriers
fc2 = round(attn2*15/40);
fc2 = 72 - fc2;
y(fc2-12:fc2-5) = zeros(8,1);
% Nulls 8 subcarriers
fc3 = round(attn3*15/40);
y(fc3-3:fc3+2) = zeros(6,1);
% Nulls 6 subcarriers
fc4 = round(attn4*15/40);
y(fc4-2:fc4+1) = zeros(4,1);
% Nulls 4 subcarriers
end
```

Bibliography

[1] Rysavy Research, "Mobile broadband capacity constraints and the need for optimization," *Rysavy Research, LLC.*, Feb 2010.

[2] Zhou Yuan, "Sidelobe suppression and agile transmission techniques for multicarrier-based cognitive radio systems," Master's thesis, Worcester Polytechnic Institute, 2009.

[3] Qing Zhao and Brian Sadler, "A survey of dynamic spectrum access," *IEEE Signal Processing Magazine*, May 2007.

[4] Ramjee Prasad, *OFDM for Wireless Communication Systems*. 2004.

[5] Wireless News. http://www.wirelessindustrynews.org/news-jan-2010/1811-012410-win-news.html, Jan 2010.

[6] Rysavy Research, "The spectrum imperative: Mobile broadband spectrum and its impacts for u.s. consumers and the economy," *Rysavy Research, LLC.*, Mar 2011.

[7] Pinyi Ren, Yichen Wang, Qinghe Du and Jing Xu, "A survey on dynamic spectrum access protocols for distributed cognitive wireless networks," *EURASIP Journal on Wireless Communications and Networking*, Feb 2012.

[8] WIMax.com. http://www.wimax.com/wimax-regulatory/what-is-unlicensed-spectrum-what-frequencies-are-they-in.

[9] Srikanth Pagadarai and Alexander Wyglinski, "A quantitative assessment of wireless spectrum measurements for dynamic spectrum access," *4th International Conference on Crowncom*, 2009.

[10] Carlos Cordeiro, Kiran Challapali and Dagnachew Birru, "IEEE 802.22: An Introduction to the First Wireless Standard based on Cognitive Radios," *Journal of Communications, Vol. 1, No. 1*, Apr 2006.

[11] CNN News. http://www.cnn.com/2011/12/14/opinion/hahn-passell-spectrum-telecoms/index.html?iref=allsearch, Dec 2011.

[12] Timo Weiss and Friedrich Jondral, "Spectrum pooling : An innovative strategy for the enhancement of spectrum efficiency," *IEEE Communications Magazine*, 2004.

[13] Joseph Mitola III, "Cognitive radio for flexible mobile multimedia communications," *IEEE International Workshop on Mobile Multimedia Communications*, 1999.

[14] Milind M. Buddhikot, "Understanding dynamic spectrum access: Models, taxonomy and challenges," *IEEE International Symposium on New Frontiers in Dynamic Spectrum Access Networks*, April 2007.

[15] Michael Marcus, "Unlicensed cognitive sharing of tv spectrum : The controversy at the federal communications commission," *IEEE Communications Magazine*, 2005.

[16] V.D.Chakravarthy, Z.Wu, A.Shaw, M.A.Temple, R.Kanna and F.Garber, "A general overlay/underlay analytic expression representing cognitive radio waveform," *Waveform Diversity and Deisgn Conference*, 2007.

[17] Rakesh Rajbanshi, Alexander M. Wyglinski and Gary J. Minden, "Peak-to-average power ratio analysis for nc-ofdm transmissions," *IEEE Vehicular Technology Conference*, pp. 1351–1355, 2007.

[18] Timo Weiss, Joerg Hillenbrand, Albert Krohn and Friedrich Jondral, "Mutual interference in ofdm-based spectrum pooling systems," *IEEE Vehicular Technology Conference*, 2004.

[19] R.Rajbanshi, A.M.Wyglinski and G.J.Minden, "An efficient implementation of the NC-OFDM transceivers for cognitive radios," *IEEE International Conference on Cognitive Radio Oriented Wireless Networks Communication*, 2006.

[20] Danijela Cabric, Ian D. ODonnell, Mike Shuo-Wei Chen and Robert W. Brodersen, "Spectrum sharing radios," *IEEE Communication Magazine*, 2006.

[21] Marcel Lopez-Rodriguez and Roger Piqueras Jover, "Resiliency of OFDM to Multipath Fading in Wireless Communications," 2007.

[22] Kaveh Pahlavan and Prashant Krishnamurthy, *Principles of Wireless Networks - A Unified Approach.* pp82, Prentice Hall, 2002.

[23] Hanna Bogucka, Alexander M. Wyglinski, Srikanth Pagadarai and Adrian Kliks, "Spectrally agile multicarrier waveforms for oppotunistic wirless access," *IEEE Communications Magazine*, June 2011.

[24] S. Pagadarai, A. Kliks, H. Bogucka, A. M. Wyglinski, "Non-contiguous multicarrier waveforms in practical opportunistic wireless systems," *IET Radar, Sonar and Navigation*, vol. 5, pp. 674 – 680, July 2011.

[25] Negin Sokhandan and Seyed Mostafa Safavi, "Sidelobe Suppression in OFDM-based Cognitive Radio Systems," *Information Sciences Signal Processing and their Applications (ISSPA)*, pp. 413 – 417, May 2010.

[26] Shih-Gu Huang and Chien-Hwa Hwang, "Improvement of active interference cancellation: Avoidance technique for ofdm cognitive radio," *IEEE Transactions on Wireless Communications*, vol. 8, December 2009.

[27] Shama Noreen and N. Z. Azeemi, "A Technique for Out-of-Band Radiation Reduction in OFDM-Based Cognitive Radio," *IEEE 17th International Conference on Telecommunications*, pp. 853 – 856, April 2010.

[28] Mahmoud S. El-Saadany, Ahmed F. Shalash and Mohamed Abdaallab, "Revisiting Active Cancellation Carriers for Shaping th Spectrum of OFDM-based Cognitive Radios," *SARNOFF*, April 2009.

[29] Paul Sutton, Baris Ozgul, Irene Macaluso and Linda Doyle, "OFDM Pulse-Shaped Waveforms for Dynamic Spectrum Access Networks," *DySPAN*, 2010.

[30] Daiming Qu, Zhiqiang Wang and Tao Jiang, "Extended active interference cancellation for sidelobe suppression in cognitive radio ofdm systems with cyclic prefix," *IEEE Transactions on Vehicular Technology*, vol. 59, May 2010.

[31] N.M. Naghsh and M.J. Omidi, "Reduction of out of band radiation using carrier-by-carrier partial response signalling in orthogonal frequency multplexing," *IET Communications*, vol. 4, January 2010.

[32] Pawel Kryszkiewicz, Hanna Bogucka and Alexander M Wyglinski, "Protection of primary users in dynamically varying radio environment: practical solutions and challenges," *EURASIP Journal on Wireless Communications and Networking*, 2012.

[33] Ivan Cosovic and Tiziano Mazzoni, "Suppression of sidelobes in OFDM systems by multiple-choice sequences," *European Transactions on Communications*, Dec 2006.

[34] Richard van Nee and Ramjee Prasad, *OFDM for Wireless Multimedia Communications*. Artech House, London, 2000.

[35] Federal Communications Commission, "Spectrum policy task force report," 2002.

[36] M. Nekovee, "Dynamic spectrum access - concepts and future achitectures," *BT Technology Journal*, vol. 24, no. 2, April 2006.

[37] Joseph Mitola III, *Cognitive Radio Architecture*. A John Wiley and Sons,INC., 2006.

[38] K. M. Markus Dillinger and N. Alonistioti, *Software Defined Radio: Architectures, Systems and Functions*. Wiley and Sons, 2003.

[39] F. K. Jondral, "Software-defined radio-basics and evolution to cognitive radio," *EURASIP Journal on Wireless Communications and Networking*, February 2005.

[40] S. S. T. Group, "New research lab leads to unique radio receiver," *E-Systems TEAM*, vol. 5, no. 4, pp. 117–123, May 1985.

[41] R. J. Lackey and D. W. Upmal, "Speakeasy: The military software radio," *IEEE Communications Magazine*, May 1995.

[42] ADT. http://adat.ch/index_e.html, July 2012.

[43] AOR. http://www.aorusa.com/receivers/ar2300.html, 2012.

[44] Woodbox Radio. http://woodboxradio.com/fdm-s1.html, Aug 2012.

[45] Elecraft. http://www.elecraft.com/KX3/kx3.htm, Oct 2012.

[46] Flex radio systems. http://www.flexradio.com/Products.aspx?topic=F5Ka_details, 2012.

[47] EPIQ Solutions. http://www.epiqsolutions.com/matchstiq/, Dec 2012.

[48] Microtelecom. http://www.microtelecom.it/perseus/, 2009.

[49] HPSDR Mercury. http://tapr.org/kits_merc.html, 2012.

[50] Ettus Research. http://www.ettus.com/products, 2012.

[51] Winradio. http://www.winradio.com/home/g31ddc.htm, 2012.

[52] NETSDR. http://www.rfspace.com/RFSPACE/NetSDR.html, 2012.

[53] Matt Ettus. Ettus Research LLC. Retrieved from. http://www.ettus.com/, 2008.

[54] Michael Joseph Leferman, "Rapid prototyping interface for software defined radio experimentation," Master's thesis, Worcester Polytechnic Institute, February 2010.

[55] Ettus Research LLC. http://code.ettus.com/redmine/ettus/projects/uhd/wiki.

[56] MathWorks. http://www.mathworks.com/products/simulink/.

[57] Y. G. Li and G. L. Stuber, *Orthogonal Frequency Division Multiplexing for Wireless Communications.* Springer, 2006.

[58] R. M. Milan Zikovic, Dominik Auras, "OFDM-based Dynamic Spectrum Access," *DySPAN*, 2010.

[59] J.-P. Linnartz and S. Hara, "Special issue on multi-carrier modulation." http://www.wirelesscommunication.nl/wireless/mccdma/mcm.html.

[60] J. A. C. Bingham, "Multicarrier modulation for data transmission - an idea whose time has come," *Communications Magazine, IEEE*, vol. 28, pp. 5–14, May 1990.

[61] J. G. Proakis and M. Salehi, *Digital Communications.* McGraw Hill Higher Education, 2008.

[62] S. B. Weinstein and Paul M. Ebert, "Data transmission by frequency-division multiplexing using the discrete fourier transform," *IEEE Transactions on Communications Technology, Vol. Com-19, No.5*, October 1971.

[63] D C Shah, B U Rindhe and S K Narayankhedkar, "Effects of cyclic prefix on ofdm system," *International Conference and Workshop on Emerging Trends in Technology*, 2010.

[64] Abraham Peled and Antonio Ruiz, "Frequency domain data transmission using reduced computational complexity algorithms," *Acoustics, Speech, and Signal Processing, IEEE International Conference in ICASSP*, April 1980.

[65] Sandro Adriano Fasolo and Carlos Augusto Rocha, "Introduction of ofdm equalization," 2006.

[66] Rakesh Rajbanshi, Alexander M. Wyglinski and Gary J. Minden, "Adaptive-mode peak-to-average power ratio reduction algorithm for ofdm-based cognitive radio," *IEEE Vehicular Technology Conference*, pp. 1–5, Sept 2006.

[67] R. Rajbanshi, *OFDM-based cognitive radio for DSA networks*. PhD thesis, University of Kansas, Lawrence, KS, USA, May 2007.

[68] Jeffrey D. Poston and William D. Horne, "Discontiguous OFDM considerations for Dynamic Spectrum Access in Idle TV Channels," *New Frontiers in Dynamic Spectrum Access Networks*, November 2005.

[69] Alexander M. Wyglisnki, "Effects of bit allocation on non-contiguous multicarrier-based cognitive radio transceivers," *Proceedings of the 64th IEEE Vehicular Technology Conference*, September 2006.

[70] Srikanth Pagadarai, "Sidelobe suppression for ofdm based cognitive radios in dynamic spectrum access networks," Master's thesis, University of Kansas, August 2007.

[71] John G. Proakis, *Digital Communications*. New York, NY, USA: McGraw Hill, 2001.

[72] A. Dhammika S. Jayalath and Chintha Tellanbura, "Reducing the out of Band Radiation of OFDM Using an Extended Guard Interval," *IEEE Vehicular Technology Conference, vol.2, pp 829-833*, October 2001.

[73] Samir Kapoor and Slobodan Nedic, "Interference Suppression in DMT Receivers using Windowing," *IEEE International Conference on Communications, vol.2, pp. 778-782*, 2000.

[74] Ivan Cosovic, Sinja Brandes and Michael Schell, "Physical layer design challenges of an ofdm based overlay system," *IST Mobile and Wireless Communications summit*, June 2006.

[75] Sinja Brandes, Ivan Cosovic and Michael Schnell, "Sidelobe suppression in OFDM systems by Insertion of Cancellation carriers," *IEEE Vehicular Technology Conference*, 2005.

[76] Srikanth Pagadarai, Rakesh Rajbanshi, Alexander M. Wyglinski and Gary J. Minden, "Sidelobe Suppression for OFDM-based Cognitive Radios Using Constellation Expansion," *Wireless Communications and Networking Conference*, 2008.

[77] Ivan Cosovic, Sinja Brandes and Michael Schnell, "Subcarrier weighting: A method for sidelobe suppression in ofdm systems," *IEEE Communications Letters, Vol. 10, No. 6*, 2006.